Journal Pre-proof

The secretome of aged fibroblasts promotes EMT-like phenotype in primary keratinocytes from elderly donors through BDNF-TrkB axis

Lavinia Tinaburri, Carola Valente, Massimo Teson, Ylenia Aura Minafò, Sonia Cordisco, Liliana Guerra, Elena Dellambra

PII: S0022-202X(20)32062-5

DOI: https://doi.org/10.1016/j.jid.2020.08.019

Reference: JID 2623

To appear in: *The Journal of Investigative Dermatology*

Received Date: 6 February 2020

Revised Date: 11 August 2020

Accepted Date: 21 August 2020

Please cite this article as: Tinaburri L, Valente C, Teson M, Minafò YA, Cordisco S, Guerra L, Dellambra E, The secretome of aged fibroblasts promotes EMT-like phenotype in primary keratinocytes from elderly donors through BDNF-TrkB axis, *The Journal of Investigative Dermatology* (2020), doi: https://doi.org/10.1016/j.jid.2020.08.019.

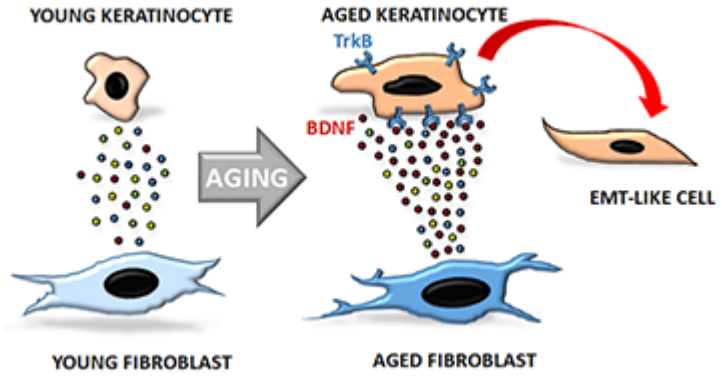

The secretome of aged fibroblasts promotes EMT-like phenotype in primary keratinocytes from elderly donors through BDNF-TrkB axis

Lavinia Tinaburri[1±], Carola Valente[1±], Massimo Teson[1], Ylenia Aura Minafò[1], Sonia Cordisco[1,2], Liliana Guerra[1] and Elena Dellambra[1*].

[1] IDI-IRCCS, Rome, Italy; [2] Department of Life, Health and Environmental Sciences, University of L'Aquila, L'Aquila, Italy.

± Equal contribution

Author emails and ORCID:		
	lavinia.tinaburri@gmail.com	0000-0001-7179-079X
	c.valente@idi.it	0000-0001-9234-2267
	m.teson@idi.it	0000-0002-7179-1255
	y.minafo@idi.it	0000-0002-3818-2837
	sonia.cordisco@tiscali.it	0000-0003-1218-847X
	l.guerra@idi.it	0000-0001-6274-6607
	e.dellambra@idi.it	0000-0002-4329-3312

Short title: Aged secretome and primary keratinocyte plasticity

Key words: aging, skin, primary keratinocytes, primary fibroblasts, secretome, EMT

Abbreviations:

3D	three-dimensional
Ab	antibody
Ctrl	control
O-SPN	supernatant from old donors
SPN	supernatant
Y-SPN	supernatant from young donors
Y-S-SPN	supernatant of senescent fibroblasts from young donors

*Corresponding author:

Dr. Elena Dellambra
Molecular and Cell Biology Laboratory,
Fondazione Luigi Maria Monti, IDI-IRCCS
Via dei Monti di Creta, 104
00167 Rome, Italy.
Phone: +39-06-66464731
E-Mail: e.dellambra@idi.it
Twitter handle: @elenadellambra

ABSTRACT

Age-related changes in the dermis can play a primary role in tumor initiation promoting the unrestrained proliferation of precancerous keratinocytes through cytokines and growth factor secretion.

We found that a high percentage of epithelial-mesenchymal transition (EMT)-like colonies raised in primary human keratinocyte cultures from old subjects after treatment with aged fibroblast supernatants (SPN). Continuous extracellular signals were required for maintaining these changes. Conversely, the secretome did not induce EMT-like colonies in keratinocytes from youngs. SPN-treated aged keratinocytes displayed the activation of pathways involved in the disjunction of cell-cell adhesion, ECM remodeling, manifestation of mesenchymal phenotype and dedifferentiation programs. Moreover, they recovered proliferation and clonogenic ability, and showed enhanced migration.

We identified an age-related increase of the BDNF secretion from fibroblasts as well as of the expression of its receptor TrkB in keratinocytes. BDNF-treatment of aged keratinocytes induces TrkB phosphorylation and recapitulated modifications promoted by aged fibroblast SPN. Furthermore, the treatment with a specific antibody against BDNF or a TrkB antagonist inhibited the paracrine signaling preventing SPN-mediated morphological and molecular changes. Finally, BDNF induced signs of matrix invasion in a 3D organotypic model.

Therefore, we demonstrate that aged fibroblast SPN promotes phenotypic plasticity in keratinocytes from the elderly through BDNF-TrkB axis.

INTRODUCTION

Squamous cell carcinoma (SCC) is one of the most common cancers worldwide and its incidence increases up to 200% accordingly to the steadily aging of the population (Ashford et al. 2017). Although aging is a major risk factor for SCC development, mechanisms underlying the relationship between skin aging and malignant transformation are not fully understood.

SCC arises "de novo" in skin or is the evolution of the “in situ” lesion, the actinic keratosis (AK). AKs and SCCs result from a multistage process comprising mutations in genes involved in epidermal homeostasis (e.g. *TP53, TP63*, *CDKN2A, PIK3CA, HRAS, NOTCH1*) and unrestrained proliferation of atypical keratinocytes. However, some AKs do not progress in SCC, even if keratinocytes have genetic or epigenetic changes. Therefore, these mutations are "permissive" of the tumour, but not enough for its onset. In fact, tumour development also need systemic or microenvironmental alterations, such as age-related changes (Ashford et al. 2017; Loaiza and Demaria 2016).

Senescent cells accumulate in aged skin (Collado et al. 2007). Cellular senescence is triggered by several stimuli that induce growth arrest and phenotypic alterations, including chromatin and secretome changes. Senescent cells acquire a pro-inflammatory status defined senescence-associated secretory phenotype (SASP) composed by growth factors, cytokines, and extracellular proteases. Thus, cellular senescence prevents the uncontrolled proliferation of damaged cells, and favours the tissue clearance and regeneration by paracrine secretion. However, the cumulative insults and the deficient clearance of damaged cells in the elderly result in senescent cell accumulation affecting tissue homeostasis and contributing to increase of cancer incidence (van Deursen 2014; Muñoz-Espín and Serrano 2014). Age-related changes in the dermis generate a highly permissible microenvironment, which allows the uncontrolled growth of mutated keratinocytes residing in normal skin, playing a primary role

in both SCC initiation and progression (Dotto 2014). Indeed, human senescent primary fibroblasts stimulate proliferation, epithelial-to-mesenchymal transition (EMT), migration and invasiveness of precancerous and malignant keratinocytes through secretion of SASP mediators (Coppe et al. 2010; Krtolica et al. 2001; Malaquin et al. 2013). Epithelial senescent cells accumulate in precancerous lesions but are not detectable after progression to malignancy. As the properties of senescent cells continuously evolve, some of them might become premalignant escaping senescence (Abbadie et al. 2017; Faget et al. 2019).

In the present study we investigate if the aged secretome of fibroblasts may modify the physiology of primary epidermal cells from elderly subjects.

RESULTS

The secretome of aged fibroblasts promotes phenotypic plasticity in keratinocytes from the elderly

Primary keratinocytes and fibroblasts from old donors display senescent features (Carlomosti et al. 2017; Cordisco et al. 2017; Cordisco et al. 2010; Tinaburri et al. 2018). Main senescent features of the strains used in present study are summarized in Figure S1. To test if the aged secretome of fibroblasts may modify the physiology of primary epidermal cells, keratinocytes from three young (<10 years) or three old (>70 years) donors were cultured with supernatants (SPNs) of fibroblasts from the same three youngs (Y-SPNs), three olds (O-SPNs) or control medium (Ctrl).

Ctrl-treated cultures from old and young subjects displayed regular keratinocyte colonies (Figure 1a,b), characterized by cells tightly adherent to each other and able to stratify. Notably, peculiar colonies appeared in SPN-treated keratinocyte cultures from old donors (Figure 1a). Conversely, no morphological changes appeared in SPN-treated keratinocytes from youngs (Figure 1b), as reported by Coppe et al. 2010. The peculiar colonies were characterized by a monolayer of elongated and irregular cells, less tightly adherent to other cells and surrounded by wide intercellular spaces, suggesting loss of cell-cell adhesion (Figure 1a). Cell morphology resembled the EMT-like phenotype of SCC cells (Rheinwald and Beckett 1981). Moreover, some regular colonies (Figure 1a, asterisk) displayed at their edge cells with EMT-like morphology (arrows) spreading outwards. Notably, the percentage of EMT-like colonies is significantly higher in aged keratinocytes treated with SPNs from old fibroblasts (Figure S2a, 60.02±5.67%) compared to that from young ones (18.03±2.98%). All analyzed strains displayed similar behavior with both SPNs from autologous or different fibroblast strains (Figure S2a-d). Interestingly, EMT-like morphology promotion is reversible. These colonies appeared within 18h after O-SPN-treatment and significantly decreased

already 3 days after, if the O-SPN was not newly added to medium (Figure S2e). Indeed, the elongated cells reacquired polygonal morphology during time.

Hallmarks of phenotypic plasticity are transdifferentiation (i.e acquisition of EMT-phenotype) and dedifferentiation (i.e acquisition of stem-like properties) that are relevant for tumor initiation (Lamouille et al. 2014). SPN-treatments induced a significant decrease of the cell-cell adhesion marker E-cadherin and increase of the mesenchymal marker vimentin in aged keratinocytes (Figure 1c) consistent with EMT promotion. This opposite protein modulation was more noticeable in O-SPN-treated cultures, according to EMT-like colony percentage. In keeping with morphology, no expression changes were observed in keratinocytes from youngs (Figure 1d).

Senescent features exhibited by aged keratinocytes include reduced clonogenic ability, precocious clonal conversion, i.e the transition from stem to transient amplifying and post-mitotic cells, and higher expression of the senescence marker p16 (Barrandon and Green 1987; Cordisco et al. 2010) (Figure S1a,c). O-SPN-treatments significantly resumed clonogenic ability (Figure 1e) and proliferation (Figure 1f), and decreased the expression of p16 and the differentiation marker involucrin (IVL) (Figure 1g) in aged keratinocytes, consistent with a dedifferentiated phenotype. Conversely, Y-SPN-treatments did not significantly affect senescence or differentiation features (Figure 1e-g).

Thus, fibroblast secretome promotes the EMT process only in keratinocytes from the elderly. These cells acquire a more relevant EMT-like phenotype and dedifferentiation features following exposure to aged secretome. The presence of continuous extracellular signals is required for maintaining morphological changes.

Brain-derived neurotrophic factor (BDNF) is a potential factor promoting phenotypic plasticity

To identify paracrine factor(s) differentially released by young and aged fibroblasts promoting cell plasticity, a secretome analysis was performed. A significant differential secretion of some SASP components was found (Figure S3a) in keeping with Waldera Lupa et al. 2015.

By the results from secretome analysis, protein association database analysis (Figure S3b) and literature data, we identified BDNF as the potential factor promoting EMT-like colonies. Indeed, BDNF secretion was significantly increased in fibroblast O-SPNs compared to Y-SPNs (Figure 2a,b). Conversely, BDNF secretion from keratinocytes was lower than that of fibroblasts and did not increase with aging (Figure S3c). Mature BDNF production results from pro-BDNF cleavage by selective metalloproteinases, such as MMP3 and MMP7 (Tajbakhsh et al. 2017). Accordingly, MMP3 secretion increased in fibroblast O-SPNs in concomitance with the decrease of metalloproteinase inhibitors (TIMPs) (Figure 2a). Modulation of both protein family in dermal fibroblasts is promoted by replicative senescence (Campisi 1998). To investigate whether also the age-related BDNF secretion could depend from cell senescence, young fibroblasts were serially cultured until they reach replicative senescence (Figure S1d). BDNF secretion increased in senescent young fibroblasts (S-Y-SPNs) compared to early passage cultures (Y-SPNs) (Figure 2b). Especially, S-Y-SPNs induced EMT-like colonies in old keratinocytes like O-SPNs (Figure 2c) strengthen the idea that fibroblast BDNF secretion was, at least in part, responsible of keratinocyte modifications.

BDNF acts through the high-affinity tropomyosin-receptor-kinase (Trk)B and the low-affinity p75 neurotrophin receptors (Tajbakhsh et al. 2017). Notably, the binding BDNF-TrkB activates pathways involved in cell-cycle progression, migration, EMT and dedifferentiation. TrkB upregulation promotes tumor progression (Moriwaki et al. 2018; Tajbakhsh et al. 2017). Expression of both receptors increased with donor age (Figure 2d,e TrkB FL). However, p75 was well-expressed in keratinocytes from youngs and its expression displayed a great variability among old individuals. Conversely, the full-length TrkB (Figure 2e TrkB FL), was

barely detectable in keratinocyte from young donors, as reported in Marconi et al. 2003, and its expression significantly increased in the elderly, suggesting that TrkB upregulation was, at least in part, responsible of cell modifications. The human TrkB gene encodes C-terminal-truncated receptors TrkB-T1 and TrkB-T-Shc that may act as dominant-negative inhibitors of the full-length receptor by preventing ligand-induced phosphorylation (Luberg et al. 2010; Thiele et al. 2009). Expression of both truncated receptors was higher in young keratinocytes and lower in old keratinocytes compared to full-length (Figure 2e). Especially, TrkB-T-Shc and full-length displayed a significant opposite modulation. TrkB is also the receptor for neurotrophin-4 (NT-4) and, in a lower affinity, neurotrophin-3 (NT-3) (Rydén and Ibáñez 1996). However, NT-3 and NT-4 secretion did not significantly vary with fibroblast aging (Figure 2a). No EMT-like colony appearance, vimentin increase or significant E-cadherin decrease have been observed following NT-treatments. Notably, NT-3-treatments even increased E-cadherin expression (Figure S3d). Indeed, ectopic expression of NT-3 in EMT-like breast-cancer cells induces E-cadherin reverting the mesenchymal phenotype to epithelial-like state (Louie et al. 2013).

BDNF promotes phenotypic plasticity in aged keratinocytes

To demonstrate the direct involvement of BDNF in cell plasticity, keratinocytes from young and elderly donors were treated with recombinant human BDNF.

A significant BDNF-dependent increase of TrkB phosphorylation and induction of EMT-like colonies (Figure 2f,g) was observed in keratinocytes from old but not from young donors (Figure S3e,f). In keeping with data obtained with O-SPN-treatments (Figure 1a, S2a-d), BDNF administration at 50ng/ml induces 76.53±4% of EMT-like colonies in aged keratinocytes (Figure 2f,g). Accordingly, BDNF-treated-aged keratinocytes displayed reduced

E-cadherin and increased vimentin (Figure 2h). BDNF-treatments also resumed proliferation and clonogenic ability (Figure 2i), and reduced p16 and IVL expression (Figure 2l).

Continuous exposure to BDNF allowed the maintenance of morphological changes and extension of keratinocyte life-span. However, cells did not indefinitely proliferate (Figure 2m). BDNF-treated keratinocytes appeared enlarged and flatten at late passage compared to early, although they still displayed EMT-like phenotype. Moreover, BDNF-treated keratinocytes were unable to grow in an anchorage-independent manner (Figure S3g). If keratinocytes were exposed to BDNF-treatment for only 7 days (BDNF rev), culture displayed a life-span similar to control, in keeping with the reversibility of morphological changes (Figure 2m).

To demonstrate the involvement of secreted BDNF in promoting EMT-like phenotype, aged keratinocytes were treated with both O-SPN and a specific antibody against human-BDNF or unrelated antibody. Unrelated-antibody-treatment did not modify O-SPN-dependent changes (Figure S3h). Conversely, anti-BDNF-antibody-treatment prevented EMT-like phenotype induced by O-SPN-treatments consistent with a block of paracrine signaling. Most of colonies (Figure 3a, O-SPN+Ab) displayed a phenotype resembling that of Ctrl and thus the EMT-like colony percentage was reduced (Figure 3b). Anti-BDNF-antibody-treatment counteracted O-SPN-dependent changes, such as cell proliferation increase (Figure 3c), E-cadherin decrease (Figure 3d, O-SPN+Ab) and vimentin increase (Figure 3e, O-SPN+Ab).

Thus, aged fibroblasts release active BDNF that induces EMT-like phenotype in aged keratinocytes.

Aged fibroblast secreted-BDNF promotes phenotypic plasticity through TrkB pathway

To demonstrate a role of BDNF-TrkB axis in promoting cell plasticity, TrkB activity was blocked by ANA-12 that selectively binds to TrkB inhibiting downstream pathways without altering TrkA and TrkC functions (Moriwaki et al. 2018).

ANA-12 prevented the EMT-like phenotype (Figure 3a, O-SPN+ANA-12), reduced the EMT-like colony percentage (Figure 3b) and counteracted proliferation (Figure 3c) in O-SPN-treated keratinocytes. ANA-12-treatment also prevented E-cadherin, p16 and IVL decrease and vimentin increase (Figure 3d-f).

Thus, secreted BDNF induces cell plasticity in aged keratinocytes through TrkB activity.

The aged secretome modulates EMT pathways similarly to BDNF-TrkB activation

To investigate the modifications of transcriptional programs in treated cells, expression of genes related to senescence and cancer stem cell was evaluated (Figure S4). Genes differentially expressed in both O-SPN and BDNF compared to Ctrl and simultaneously expressed in opposite direction in O-SPN+ANA-12 are reported in Figure S5a. The GO and KEGG pathway analysis evidenced mainly genes related to Pathways in Cancer (red spheres) and to Regulation of developmental process (blue spheres), which is orchestrated by pathways involved in phenotypic plasticity (Figure S5b,c). Among them, pathways downstream to TrkB or related to epidermal stem cell properties were highlighted (Figure 4a).

The BDNF-TrkB axis acts through several intracellular signaling, such as Ras/MAPK, PI3K/Akt, and Jak2/STAT3 pathways. Their cross-talk activates the downstream EMT master genes (i.e Snail (SNAI1), Slug (SNAI2), Twist-related protein 1 (TWIST1), zinc-finger E-box-binding homeobox (ZEB)1 and ZEB2) that directly down-regulate E-cadherin expression and activate genes associated with mesenchymal phenotype and cell-matrix adhesion (i.e integrins, mainly β1 subunit, and ECM components, including collagens and fibronectin) enhancing pro-migratory pathways (Lamouille et al. 2014). Glycogen synthase kinase-3β

(GSK3β) inhibits EMT and tumor invasion by inactivation of Snail transcriptional activity. Notably, Akt inhibits GSK3β activity by phosphorylation and, in turn, stabilizes Snail (Cross et al. 1995). Akt also mediates a negative control of p53 levels resulting in ZEB induction and SASP increase (Coppe et al. 2010).

Beyond the transcriptional modulation, the expression levels and the phosphorylation status of TrkB downstream targets following O-SPN or BDNF-treatments were consistent with the activation of PI3K/Akt pathway and the consequent GSK3β inhibition and p53 decrease, as well as the activation of Jak/STAT3 and ERK1/2 (MAPK42/44) pathways (Figure 4b). Conversely, ANA-12-treatments counteracted the O-SPN-mediated activations (Figure 4b). Accordingly, the transcript expression of EMT master genes (Figure 4a and S6a), cell-matrix adhesion genes and mesenchymal markers (Figure 4a) significantly increased in O-SPN- or BDNF-treated cultures and was prevented by ANA-12.

Thus, O-SPN promotes the activation of downstream TrkB pathways similarly to BDNF.

The aged secretome modulates dedifferentiation pathways similarly to BDNF-TrkB activation.

Cell-cell junctions inhibit proliferation by Hippo pathway. The loss of E-cadherin and β-catenin induces proliferation and acquisition of stem-like properties by activation of the transcriptional coactivator Yes-associated protein (YAP) and its paralog TAZ (Kim et al. 2011; Zanconato et al. 2019). Indeed, YAP promotes an undifferentiated state by DLL1-mediated inhibition of Notch1 pro-differentiation signaling (Negri et al. 2019; Totaro et al. 2017). According to E-cadherin and β-catenin modulation, some effectors of the Hippo pathways, such as the YAP, TAZ and their target serpin E1, were differentially expressed in treated-keratinocytes (Figure 4a). p53 and YAP regulate the transcription of Notch1 and the Notch-inhibitor DLL1, respectively (Lefort et al. 2007; Totaro et al. 2017). In agreement with

p53 expression, Notch1 transcript was significantly downregulated in O-SPN- or BDNF-treated cells and its decrease was prevented by ANA-12. Its pro-differentiation ligands DLL4 and JAG1 followed a similar trend whereas the Notch-inhibitor DLL1 displayed an opposite expression consistent with YAP modulation (Figure 4a).

In Ctrl colonies (Figure 4c), membrane-bound-β-catenin was mainly localized at cell-cell contact as E-cadherin. Nuclear (active) YAP was localized in peripheral proliferating cells and cytoplasmic (inactive) form in the central differentiated cells. Like SCCs, EMT-like colonies displayed significant decrease of membrane-bound-β-catenin (Figure 4b,c) with a discontinuous pattern (Figure S6b) and mainly nuclear YAP expression. β-catenin reduction and YAP nuclear translocation were prevented by ANA-12.

As expected, DLL1 and Notch1 were localized in membrane at the cell–cell interface and in the cytoplasm of Ctrl and O-SPN+ANA-12-treated colonies. In EMT-like colonies DLL1 displayed cytoplasmic and perinuclear localization. Notch1 was mainly cytoplasmic and associated with vesicles distributed throughout the cytoplasm and accumulated in perinuclear region (> 80%) (Figure 4c and S6c) suggesting an increased receptor degradation by the endocytic pathway. Indeed, this pattern was similar to those observed following GSK3β silencing/inhibition, which increases the recycling rate of the receptor (Zheng and Conner 2018).

Thus, O-SPN promotes the modulation of dedifferentiation pathways similarly to BDNF. The loss of adhesion molecules and the spreading of EMT-like cells can activate YAP and promote that undifferentiated state.

The BDNF-TrkB axis promotes migration in aged keratinocytes

Migration ability is a crucial feature of cells starting the EMT program (Lamouille et al. 2014). To investigate the migration of treated aged keratinocytes, the gap closure of cell-free

areas was monitored taking pictures at different time points (Figure 5a). A significant early gap closure was seen in O-SPN- or BDNF-treated cultures compared to Ctrl whereas ANA-12 significantly slows down the migratory effect induced by O-SPN-treatment.

Thus, BDNF-TrkB axis activation promotes a pro-migratory effect in aged keratinocytes.

BDNF induces signs of matrix invasion in a 3D organotypic model composed by aged fibroblasts and keratinocytes

Carcinoma-associated fibroblasts (CAF) remodel the tumor microenvironment playing an active role in cancer development (Albrengues et al. 2015). The invasiveness of treated aged keratinocytes was investigated in a 3D organotypic skin model (Figure S7a,b). CAFs display higher levels of the main marker alpha-smooth muscle actin (α-SMA) (LeBleu and Kalluri 2018), plasminogen activator inhibitor-1 (PAI-1/SerpinE), BDNF and VEGF-C compared to old fibroblasts (Figure S7c,d). Notably, PAI-1 release facilitates the SCC invasiveness and BDNF promotes VEGF-C-dependent lymphangiogenesis (Freytag et al. 2009; Jiffar et al. 2017; Lin et al. 2017).Vimentin, which is expressed by overall fibroblast populations, did not significantly vary. Moreover, matrix-embedded CAFs display contractile properties (Figure S7e).

As shown in Figure 5b, SCC13 cells invaded the matrix containing CAFs or aged fibroblasts (OldF), although the Invasion Index (I.I) was lower in the latter condition. The I.I was increased by BDNF-treatment and reduced by ANA-12 in both conditions. Notably, ANA-12-treatments were able to modify cell morphology and increase E-cadherin in SCC-13 culture (Figure 5c). Moreover, vimentin, which is barely detectable, was down-modulated. ANA-12 induced also SCC13 differentiation in 3D model (Figure S7f).

Aged keratinocytes (OldK) did not show invasive capacity in the matrix containing aged fibroblasts (OldF) (Figure 5d and S7f). Notably, BDNF-treatment induced keratinocyte

hyperplasia and some epidermal areas growing inwards the matrix. When matrix contained CAFs, few aged keratinocytes (arrow) slightly grew inwards. BDNF-treatment increased this phenomenon. ANA-12-treatment induced cell differentiation in both conditions.

Thus, the epidermal compartment generated by aged keratinocytes is able to grow inwards the matrix in presence of CAFs or BDNF. Conversely, keratinocytes from young donors (Figure S7f, YoungK) did not invade the matrix neither with CAFs nor with BDNF. Moreover, SCC did not invade the matrix containing young fibroblasts (SCC13/YoungF).

DISCUSSION

Since aging is a major risk factor for SCC development, understanding the mechanisms that link skin aging and malignant transformation is crucial for developing preventive therapies. Senescent cells accumulate in aged tissues modifying their properties following microenvironmental stimuli and, therefore, some of them might become premalignant (Abbadie et al. 2017; Dotto 2014; Faget et al. 2019).

Our results demonstrate that the secretome of aged fibroblasts modifies the morphology of aged keratinocytes that become characterized by features associated to phenotypic plasticity and relevant for tumor initiation. The presence of continuous extracellular signals is required for maintaining EMT-like morphology. The reversibility of the EMT process by signaling suspension is important for the colonization of other tissues (Hanahan and Weinberg 2011). To our knowledge, this is the first demonstration that aged fibroblast secretome promotes EMT and dedifferentiation programs on primary aged keratinocytes.

BDNF-TrkB activation and EMT-like phenotype

BDNF-TrkB axis is a critical signaling that promotes EMT, as well as the migration and invasion of epithelial malignancies (Kupferman et al. 2010; Moriwaki et al. 2018; Tajbakhsh et al. 2017; Thiele et al. 2009).

We demonstrate that the BDNF-TrkB axis is a cross-talk signaling involved in EMT-like promotion of aged keratinocytes. BDNF secretion grows with skin aging and is related to fibroblast senescence. Full-length TrkB expression increases with aging whereas TrkB-T-Shc isoform, which may have dominant-negative effects, decreases. Furthermore, BDNF-treatment induces TrkB phosphorylation and recapitulates O-SPN-mediated morphological and molecular modifications in aged keratinocytes. BDNF- and O-SPN-treated cultures exhibit activation of TrkB downstream pathways that sustain proliferative signaling and promote EMT program. Accordingly, treated cultures are characterized by decreased

expression of the cell-cell adhesion proteins, modification of shape, increased expression of mesenchymal markers and cell-matrix adhesion proteins, enhanced proliferation and migration. Finally, TrkB signaling inhibition prevents O-SPN-mediated changes.

BDNF-TrkB activation and dedifferentiation

Genes involved in phenotypic plasticity and related to cancer stem cells are differentially expressed in treated keratinocytes. Interestingly, some of them (e.g *TP53, CDKN2A, PIK3CA, YAP1, NOTCH1*) control the balance between self-renewal and senescence/differentiation, and are mutated in AK and SCC (Ashford et al. 2017).

p16 inhibition and enforced YAP in keratinocytes results in extension of their lifespan by blocking clonal conversion (Maurelli et al. 2006; De Rosa et al. 2019). EMT master genes can directly regulate senescence through p16 down-regulation in early steps of tumorigenesis (Cakouros et al. 2012; Smit and Peeper 2010). EMT itself may promote the activation of YAP that acts as nuclear relays of mechanical signals exerted by ECM rigidity, cell density and shape modifications to regulate cell fate (Totaro et al. 2017). Perturbation of E-cadherin/catenin complex activates YAP that promotes proliferation and stem-like phenotype through DLL1-mediated Notch inhibition (Negri et al. 2019; Totaro et al. 2017; Zanconato et al. 2019). The tumor suppressor Notch1 induces early differentiation markers, such as involucrin (Rangarajan et al. 2001) and its interaction with DLL1 results in cis-inhibition of Notch signaling that, in turn, protects the undifferentiated cell state by receptor degradation (Negri et al. 2019; Totaro et al. 2017). Aging, inflammation or tissue damage alter mechanical homeostasis or induce ECM stiffening lowering the threshold for YAP activation (Zanconato et al. 2019).

In EMT-like colonies, YAP and Notch1 are modulated in agreement to a dedifferentiated phenotype as well as the decreased expression of adhesion molecules, p16 and involucrin. Those shape and expression modulations are prevented by TrkB signaling inhibition.

Continuous exposure to BDNF allow an extension of keratinocyte life-span in keeping with p16 and p53 down-regulation and YAP activation. However, keratinocytes do not by pass the second senescence barrier (or crisis) that can be overcome by maintenance of telomere length (Hanahan and Weinberg 2011). Notably, telomerase expression does not increase following treatments.

BDNF-TrkB activation and tumor promotion

A critical importance of BDNF-TrkB signaling in the tumor microenvironment is emerging. CAF-derived BDNF contribute to create a pro-invasive and pro-metastatic microenvironment through paracrine signaling. Interestingly, fibroblasts are converted to CAFs by SCC co-colturing and, in turn, they release increased levels of BNDF (Dudás et al. 2011; Jiffar et al. 2017). Although BDNF-treated keratinocytes are not able to undergo immortalization and anchorage-independent growth, we provide evidence that the epidermal compartment generated by aged keratinocytes is competent to invade the matrix in presence of CAFs or BDNF in organotypic cultures. In both conditions reconstructed epidermis displays cellular hyperplasia that is a common pre-neoplastic response to specific stimuli and can be reverted if the stimulus is removed (Ashford et al. 2017). Notably, Yap1 activation leads to epidermal hyperplasia and multiple epidermal invaginations into the dermis of mice resembling *in situ* SCC (Schlegelmilch et al. 2011).

Thus, aged keratinocytes are responsive to microenvironment changes and BDNF increase different from young keratinocytes, indicating that TrkB activation play a key role in inducing pre-neoplastic features. However, subsequent genetic and/or epigenetic hits are required for undergoing to a full matrix invasion. The epidermal compartment generated by SCC invade the matrix containing CAFs or aged fibroblasts but not young fibroblasts. Thus, our data support the view that a permissive environment is important for SCC development and that normal microenvironment has tumor suppressive properties (Dotto 2014; Hanahan and

Weinberg 2011; Lim and South 2014; Whitson and Oro 2017). Furthermore, TrkB signaling inhibition reverts EMT and pro-invasive properties of SCC cells. Thus, BDNF-TrkB activation may be a critical step of the multistage progression towards SCC and a possible target for therapeutically preventing SCC invasion or relapse.

Altogether our findings demonstrate that aged fibroblast SPN promotes phenotypic plasticity in keratinocytes from the elderly through BDNF-TrkB axis.

MATERIALS AND METHODS

Detailed descriptions are provided in Supplementary Materials and Methods.

Cell cultures

Following written informed consent, keratinocytes and fibroblasts were obtained from skin biopsies and cultivated on feeder-layer of lethally irradiated 3T3-J2 cells. 3T3-J2 (a gift from prof. Howard Green, Boston, MA), primary human keratinocytes and fibroblasts were grown as described previously (Panacchia et al. 2010; Rheinwald and Green 1975). CAFs isolated from patients with SCC were grown in DMEM-10% FCS. SCC cells (a gift from James Rheinwald, Boston, MA) were grown as described previously (Rheinwald and Beckett 1981). Procedures were performed under our institutional ethical committee approval and in adherence with the principles of the Declaration of Helsinki.

Culture treatments

SPNs were obtained from primary fibroblasts (70% of confluence) cultured in DMEM-glutamine for 72h. Human recombinant-BDNF, anti-human-BDNF (Sigma-Aldrich) and ANA-12 (Cayman Chemical) were used at the final concentration of 50ng/ml, 1µg/ml and 50µM, respectively.

Secretome analysis

SPNs were submitted to biotin-label-based antibody arrays for profiling protein secretion (RayBiothec).

Quantitative RT-PCR, Immunofluorescence and Immunoblots

Assays were performed as described in Maurelli et al. 2016. Primers are shown in TableS1. Antibodies are shown in TableS2.

Proliferation and migration assay

Assays were performed by the Click-iT® EdU Alexa Fluor® 488 Imaging Kit (Thermo Fisher) and OrisTM Cell Migration Kit (Platypus Technologies).

Organotypic invasion assays

Fibroblasts or CAFs were embedded in matrix gels. Gels were overlaid with SCC13 cells or primary keratinocytes. 3D models were lifted at the cell-air-interface 24h later and treated for 5 days.

Statistical analysis

Data were expressed as mean±standard deviation (s.d). Statistical analysis was performed by the Student's t-test.

DATA AVAILABILITY

Datasets related to this article can be found in the Supplementary Materials.

CONFLICT OF INTEREST

The authors declare no conflict of interest.

ACKNOWLEDGMENTS

This research was supported by grants from the Italian Ministry of Health (Ricerca corrente, RF-IDI-2008-1224652 and RF2016-02362541) (E.D.). We are grateful to Dr.s N. De Luca, A.L. Severi and F. Gangi (IDI-IRCCS, Rome) for technical assistance.

AUTHOR CONTRIBUTION

Conceptualization: ED; Formal Analysis: LT, CV, YAM, SC, LG, ED; Funding Acquisition: ED; Investigation: LT, CV, MT, YAM, SC, ED; Project Administration: ED; Writing - Original Draft Preparation: ED; Writing - Review and Editing: LG, ED.

REFERENCES

Abbadie C, Pluquet O, Pourtier A. Epithelial cell senescence: an adaptive response to pre-carcinogenic stresses? Cell. Mol. Life Sci. 2017;74(24):4471–509 Available from: http://link.springer.com/10.1007/s00018-017-2587-9

Albrengues J, Bertero T, Grasset E, Bonan S, Maiel M, Bourget I, et al. Epigenetic switch drives the conversion of fibroblasts into proinvasive cancer-associated fibroblasts. Nat. Commun. Nature Publishing Group; 2015;6:1–15 Available from: http://dx.doi.org/10.1038/ncomms10204

Ashford BG, Clark J, Gupta R, Iyer NG, Yu B, Ranson M. Reviewing the genetic alterations in high-risk cutaneous squamous cell carcinoma: A search for prognostic markers and therapeutic targets. Head Neck. 2017;39(7):1462–9 Available from: http://doi.wiley.com/10.1002/hed.24765

Barrandon Y, Green H. Three clonal types of keratinocyte with different capacities for multiplication. Proc. Natl. Acad. Sci. U. S. A. 1987;84(8):2302–6 Available from: http://www.pnas.org/content/84/8/2302.short

Cakouros D, Isenmann S, Cooper L, Zannettino A, Anderson P, Glackin C, et al. Twist-1 induces Ezh2 recruitment regulating histone methylation along the Ink4A/Arf locus in mesenchymal stem cells. Mol. Cell. Biol. 2012;32(8):1433–41 Available from: http://www.ncbi.nlm.nih.gov/pubmed/22290439

Campisi J. The role of cellular senescence in skin aging. J. Investig. Dermatol. Symp. Proc. Elsevier Masson SAS; 1998;3(1):1–5 Available from: http://www.ncbi.nlm.nih.gov/pubmed/9732048

Carlomosti F, D'Agostino M, Beji S, Torcinaro A, Rizzi R, Zaccagnini G, et al. Oxidative Stress-Induced miR-200c Disrupts the Regulatory Loop Among SIRT1, FOXO1, and eNOS. Antioxid. Redox Signal. 2017;27(6):328–44 Available from:

http://online.liebertpub.com/doi/10.1089/ars.2016.6643

Collado M, Blasco M a, Serrano M. Cellular senescence in cancer and aging. Cell. 2007;130(2):223–33 Available from: http://www.ncbi.nlm.nih.gov/pubmed/17662938

Coppe JP, Desprez PY, Krtolica A, Campisi J. The senescence-associated secretory phenotype: the dark side of tumor suppression. Annu Rev Pathol. 2010;5:99–118 Available from: https://www.ncbi.nlm.nih.gov/pubmed/20078217

Cordisco S, Magenta A, Briganti S, Teson M, Castiglia D, Dellambra E, et al. Accelerated features of senescence in cultured type 2 diabetic skin fibroblasts. Eur. J. Dermatology. 2017;27(4):408–10 Available from: http://www.john-libbey-eurotext.fr/medline.md?doi=10.1684/ejd.2017.3020

Cordisco S, Maurelli R, Bondanza S, Stefanini M, Zambruno G, Guerra L, et al. Bmi-1 reduction plays a key role in physiological and premature aging of primary human keratinocytes. J. Invest. Dermatol. 2010;130(4):1048–62

Cross DAE, Alessi DR, Cohen P, Andjelkovich M, Hemmings BA. Inhibition of glycogen synthase kinase-3 by insulin mediated by protein kinase B. Nature. 1995;378(6559):785–9 Available from: http://www.nature.com/articles/378785a0

De Rosa L, Secone Seconetti A, De Santis G, Pellacani G, Hirsch T, Rothoeft T, et al. Laminin 332-Dependent YAP Dysregulation Depletes Epidermal Stem Cells in Junctional Epidermolysis Bullosa. Cell Rep. ElsevierCompany.; 2019;27(7):2036–2049.e6 Available from: https://doi.org/10.1016/j.celrep.2019.04.055

Dotto GP. Multifocal epithelial tumors and field cancerization: Stroma as a primary determinant. J. Clin. Invest. 2014;124(4):1446–53

Dudás J, Bitsche M, Schartinger V, Falkeis C, Sprinzl GM, Riechelmann H. Fibroblasts produce brain-derived neurotrophic factor and induce mesenchymal transition of oral

tumor cells. Oral Oncol. 2011;47(2):98–103

Faget D V, Ren Q, Stewart SA. Unmasking senescence: context-dependent effects of SASP in cancer. Nat. Rev. Cancer. 2019;19(8):439–53 Available from: http://www.ncbi.nlm.nih.gov/pubmed/31235879

Freytag J, Wilkins-Port CE, Higgins CE, Carlson JA, Noel A, Foidart J-M, et al. PAI-1 Regulates the Invasive Phenotype in Human Cutaneous Squamous Cell Carcinoma. J. Oncol. 2009;2009:1–12 Available from: http://www.pubmedcentral.nih.gov/articlerender.fcgi?artid=2829771&tool=pmcentrez&rendertype=abstract

Hanahan D, Weinberg R a. Hallmarks of cancer: the next generation. Cell. Elsevier Inc.; 2011;144(5):646–74 Available from: http://www.ncbi.nlm.nih.gov/pubmed/21376230

Jiffar T, Yilmaz T, Lee J, Miller Y, Feng L, El-Naggar A, et al. Brain derived neutrophic factor (BDNF) coordinates lympho-vascular metastasis through a fibroblast-governed paracrine axis in the tumor microenvironment. Cancer cell Microenviron. 2017;4(2) Available from: http://www.smartscitech.com/index.php/CCM/article/view/1566

Kim NG, Koh E, Chen X, Gumbiner BM. E-cadherin mediates contact inhibition of proliferation through Hippo signaling-pathway components. Proc. Natl. Acad. Sci. U. S. A. 2011;108(29):11930–5

Krtolica A, Parrinello S, Lockett S, Desprez P-Y, Campisi J. Senescent fibroblasts promote epithelial cell growth and tumorigenesis: A link between cancer and aging. Proc. Natl. Acad. Sci. 2001;98(21):12072–7 Available from: http://www.pnas.org/cgi/doi/10.1073/pnas.211053698

Kupferman ME, Jiffar T, El-Naggar A, Yilmaz T, Zhou G, Xie T, et al. TrkB induces

EMT and has a key role in invasion of head and neck squamous cell carcinoma. Oncogene. 2010;29(14):2047–59 Available from: http://linkinghub.elsevier.com/retrieve/pii/S0022202X15370834

Lamouille S, Xu J, Derynck R. Molecular mechanisms of epithelial-mesenchymal transition. Natl. Rev. Mol. Cell Biol. 2014;15(3):178–96

LeBleu VS, Kalluri R. A peek into cancer-associated fibroblasts: Origins, functions and translational impact. DMM Dis. Model. Mech. 2018;11(4):1–9

Lefort K, Mandinova A, Ostano P, Kolev V, Calpini V, Kolfschoten I, et al. Notch1 is a p53 target gene involved in human keratinocyte tumor suppression through negative regulation of ROCK1/2 and MRCK kinases. Genes Dev. 2007;21(5):562–77 Available from: http://www.genesdev.org/cgi/doi/10.1101/gad.1484707

Lim YZ, South AP. Tumour-stroma crosstalk in the development of squamous cell carcinoma. Int. J. Biochem. Cell Biol. 2014;53:450–8 Available from: http://www.ncbi.nlm.nih.gov/pubmed/24955488

Lin C-Y, Wang S-W, Chen Y-L, Chou W-Y, Lin T-Y, Chen W-C, et al. Brain-derived neurotrophic factor promotes VEGF-C-dependent lymphangiogenesis by suppressing miR-624-3p in human chondrosarcoma cells. Cell Death Dis. 2017;8(8):e2964 Available from: http://www.nature.com/doifinder/10.1038/cddis.2017.354

Loaiza N, Demaria M. Cellular senescence and tumor promotion: Is aging the key? Biochim. Biophys. Acta. Elsevier B.V.; 2016;1865(2):155–67 Available from: http://dx.doi.org/10.1016/j.bbcan.2016.01.007

Louie E, Chen XF, Coomes A, Ji K, Tsirka S, Chen EI. Neurotrophin-3 modulates breast cancer cells and the microenvironment to promote the growth of breast cancer brain metastasis. Oncogene. 2013;32(35):4064–77 Available from: https://www.ncbi.nlm.nih.gov/pmc/articles/PMC3624763/pdf/nihms412728.pdf

Luberg K, Wong J, Weickert CS, Timmusk T. Human TrkB gene: Novel alternative transcripts, protein isoforms and expression pattern in the prefrontal cerebral cortex during postnatal development. J. Neurochem. 2010;113(4):952–64

Malaquin N, Vercamer C, Bouali F, Martien S, Deruy E, Wernert N, et al. Senescent Fibroblasts Enhance Early Skin Carcinogenic Events via a Paracrine MMP-PAR-1 Axis. Eckert RL, editor. PLoS One. 2013;8(5):e63607 Available from: https://dx.plos.org/10.1371/journal.pone.0063607

Marconi A, Terracina M, Fila C, Franchi J, Bonté F, Romagnoli G, et al. Expression and Function of Neurotrophins and Their Receptors in Cultured Human Keratinocytes. J. Invest. Dermatol. 2003;121(6):1515–21

Maurelli R, Tinaburri L, Gangi F, Bondanza S, Severi AL, Scarponi C, et al. The role of oncogenic Ras in human skin tumorigenesis depends on the clonogenic potential of the founding keratinocytes. J. Cell Sci. 2016;129(5):1003–17 Available from: http://jcs.biologists.org/cgi/doi/10.1242/jcs.176842

Maurelli R, Zambruno G, Guerra L, Abbruzzese C, Dimri G, Gellini M, et al. Inactivation of p16 INK4a (inhibitor of cyclin-dependent kinase 4A) immortalizes primary human keratinocytes by maintaining cells in the stem cell compartment. FASEB J. 2006;20(9):1516–8 Available from: http://www.ncbi.nlm.nih.gov/pubmed/16754749

Moriwaki K, Ayani Y, Kuwabara H, Terada T, Kawata R, Asahi M. TRKB tyrosine kinase receptor is a potential therapeutic target for poorly differentiated oral squamous cell carcinoma. Oncotarget. 2018;9(38):25225–43 Available from: http://www.oncotarget.com/fulltext/25396%0Ahttp://www.ncbi.nlm.nih.gov/pubmed/29861866%0Ahttp://www.pubmedcentral.nih.gov/articlerender.fcgi?artid=PMC5982746

Muñoz-Espín D, Serrano M. Cellular senescence: from physiology to pathology. Nat. Rev. Mol. Cell Biol. Nature Publishing Group; 2014;15(7):482–96 Available from: http://www.ncbi.nlm.nih.gov/pubmed/24954210

Negri VA, Logtenberg MEW, Renz LM, Oules B, Walko G, Watt FM. Delta-like 1-mediated cis-inhibition of Jagged1/2 signalling inhibits differentiation of human epidermal cells in culture. Sci. Rep. 2019;9(1):1–11

Panacchia L, Dellambra E, Bondanza S, Paterna P, Maurelli R, Paionni E, et al. Nonirradiated human fibroblasts and irradiated 3T3-J2 murine fibroblasts as a feeder layer for keratinocyte growth and differentiation in vitro on a fibrin substrate. Cells. Tissues. Organs. 2010;191(1):21–35 Available from: http://www.ncbi.nlm.nih.gov/pubmed/19546512

Rangarajan A, Talora C, Okuyama R, Nicolas M, Mammucari C, Oh H, et al. Notch signaling is a direct determinant of keratinocyte growth arrest and entry into differentiation. EMBO J. 2001;20(13):3427–36 Available from: http://www.ncbi.nlm.nih.gov/pubmed/11432830

Rheinwald JG, Beckett MA. Tumorigenic keratinocyte lines requiring anchorage and fibroblast support cultured from human squamous cell carcinomas. Cancer Res. 1981;41(5):1657–63 Available from: http://www.ncbi.nlm.nih.gov/pubmed/7214336

Rheinwald JG, Green H. Serial cultivation of strains of human epidermal keratinocytes: the formation of keratinizing colonies from single cells. Cell. 1975;6(3):331–43 Available from: http://www.ncbi.nlm.nih.gov/pubmed/1052771

Rydén M, Ibáñez CF. Binding of Neurotrophin-3 to p75, TrkA, and TrkB Mediated by a Single Functional Epitope Distinct from That Recognized by TrkC. J. Biol. Chem. 1996;271(10):5623–7 Available from: http://www.jbc.org/lookup/doi/10.1074/jbc.271.10.5623

Schlegelmilch K, Mohseni M, Kirak O, Pruszak J, Rodriguez JR, Zhou D, et al. Yap1 Acts Downstream of α-Catenin to Control Epidermal Proliferation. Cell. 2011;144(5):782–95 Available from: https://www.ncbi.nlm.nih.gov/pmc/articles/PMC3624763/pdf/nihms412728.pdf

Smit M, Peeper D. Epithelial-mesenchymal transition and senescence: two cancer-related processes are crossing paths. Aging (Albany NY). 2010;2(1):5–11 Available from: http://www.ncbi.nlm.nih.gov/pmc/articles/PMC2993803/

Tajbakhsh A, Mokhtari-Zaer A, Rezaee M, Afzaljavan F, Rivandi M, Hassanian SM, et al. Therapeutic Potentials of BDNF/TrkB in Breast Cancer; Current Status and Perspectives. J. Cell. Biochem. 2017;118(9):2502–15

Thiele CJ, Li Z, McKee AE. On Trk - the TrkB signal transduction pathway is an increasingly important target in cancer biology. Clin. Cancer Res. 2009;15(19):5962–7

Tinaburri L, D'Errico M, Sileno S, Maurelli R, Degan P, Magenta A, et al. miR-200a Modulates the Expression of the DNA Repair Protein OGG1 Playing a Role in Aging of Primary Human Keratinocytes. Oxid. Med. Cell. Longev. 2018;2018:1–17 Available from: https://www.hindawi.com/journals/omcl/2018/9147326/

Totaro A, Castellan M, Battilana G, Zanconato F, Azzolin L, Giulitti S, et al. YAP/TAZ link cell mechanics to Notch signalling to control epidermal stem cell fate. Nat. Commun. Nature Publishing Group; 2017;8(May):15206 Available from: http://www.nature.com/doifinder/10.1038/ncomms15206

van Deursen JM. The role of senescent cells in ageing. Nature. Nature Publishing Group; 2014;509(7501):439–46 Available from: http://www.ncbi.nlm.nih.gov/pubmed/24848057

Waldera Lupa DM, Kalfalah F, Safferling K, Boukamp P, Poschmann G, Volpi E, et al.

Characterization of Skin Aging-Associated Secreted Proteins (SAASP) Produced by Dermal Fibroblasts Isolated from Intrinsically Aged Human Skin. J. Invest. Dermatol. Elsevier Masson SAS; 2015;135(8):1954–68 Available from: http://dx.doi.org/10.1038/jid.2015.120

Whitson RJ, Oro AE. Soil Primes the Seed: Epigenetic Landscape Drives Tumor Behavior. Cell Stem Cell. Elsevier; 2017;20(2):149–50 Available from: http://linkinghub.elsevier.com/retrieve/pii/S1934590917300085

Zanconato F, Cordenonsi M, Piccolo S. YAP and TAZ: a signalling hub of the tumour microenvironment. Nat. Rev. Cancer. Springer US; 2019;19(AUGUST):454–64 Available from: http://dx.doi.org/10.1038/s41568-019-0168-y

Zheng L, Conner SD. Glycogen synthase kinase 3β inhibition enhances Notch1 recycling. Mol. Biol. Cell. 2018;29(4):389–95

Figure 1

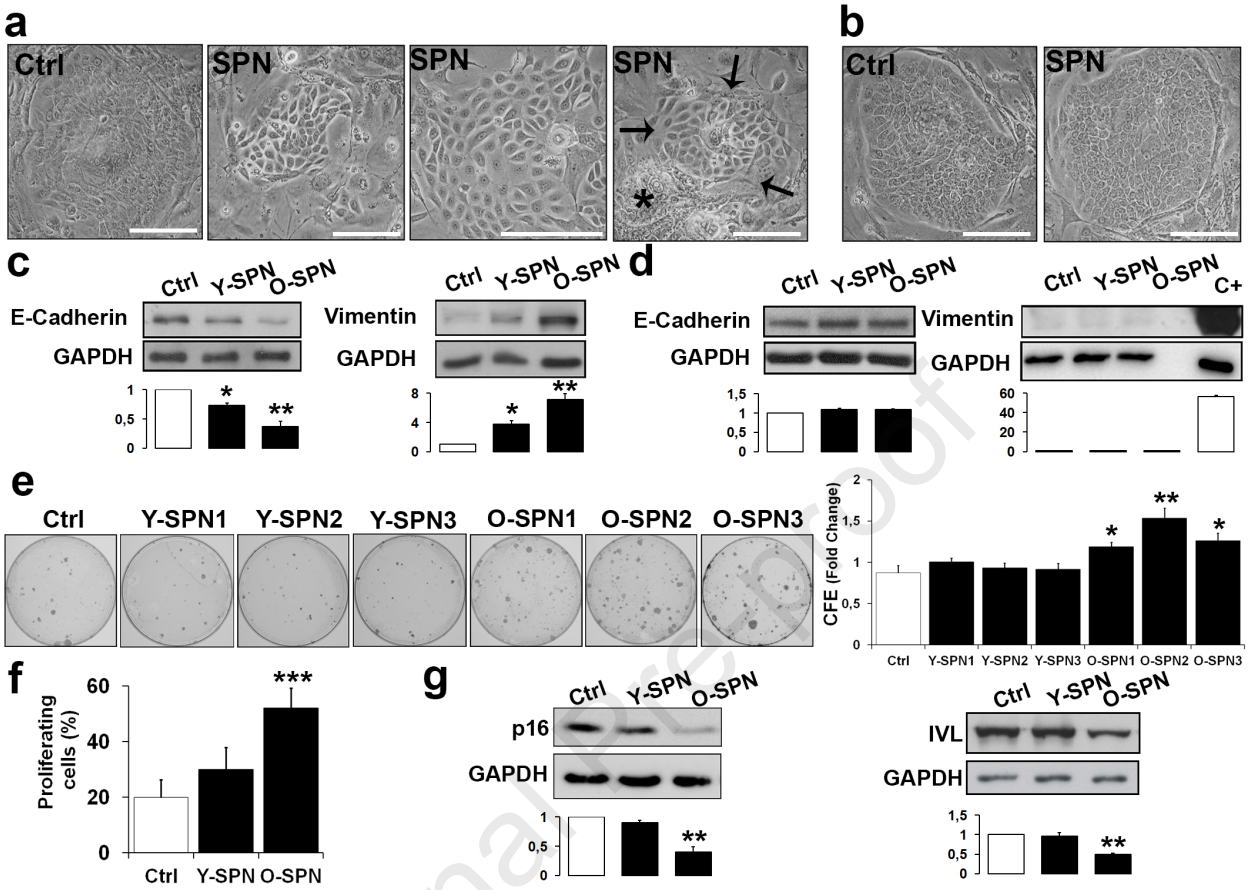

Figure 2

a

Protein	*Y-SPN*	*O-SPN*	*p*
BDNF	0.21±0.19	4.95±1.05	0.0001
MMP3	3.65±1.51	6.81±0.97	0.002
TIMP1	6.95±1.03	3.91±1.05	0.001
TIMP2	7.20±1.61	3.61±1.26	0.002
TIMP4	0.37±0.05	0.17±0.18	0.04
NT3	0.03±0.05	0.11±0.11	0.14
NT4	-	0.10±0.12	0.10

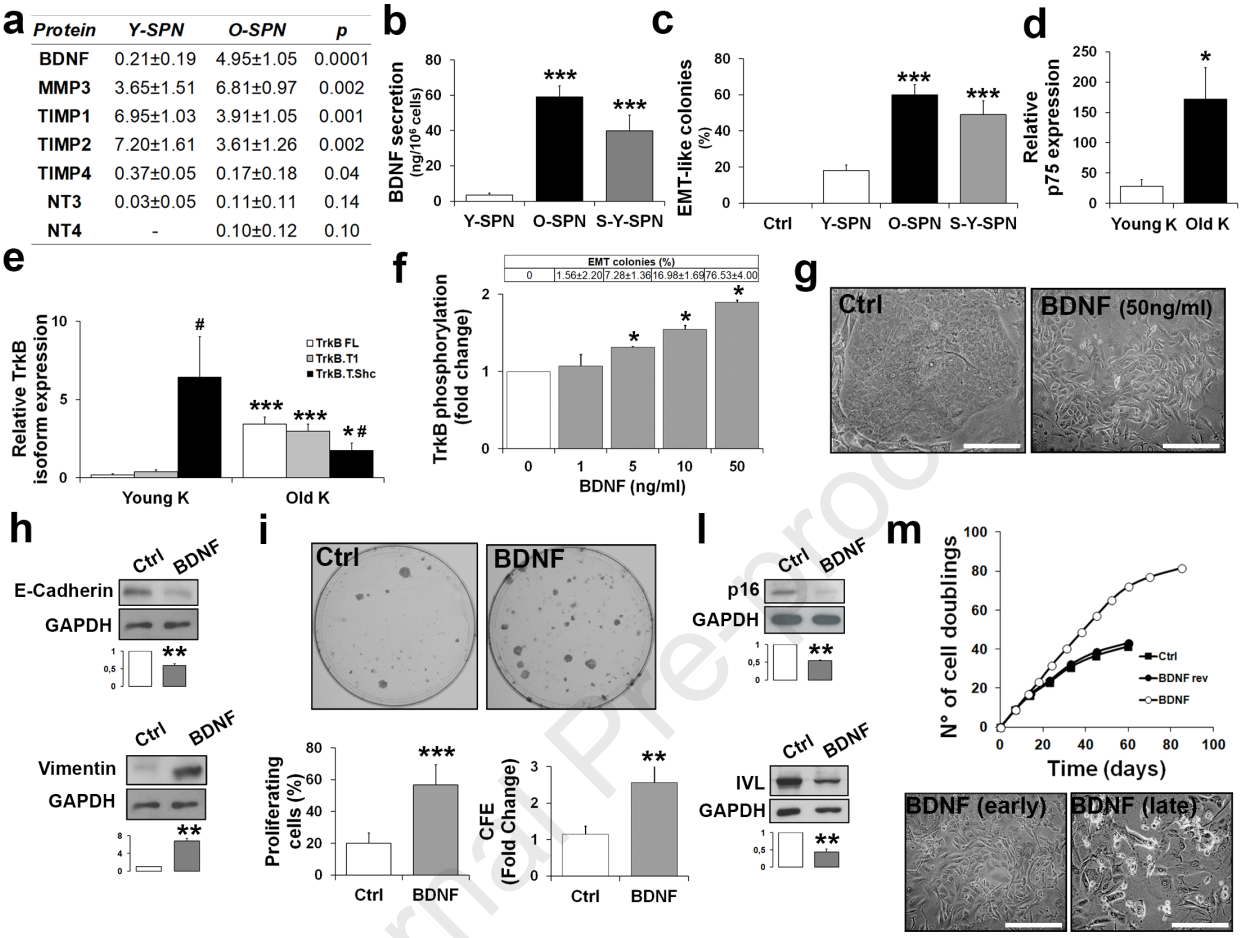

Figure 3

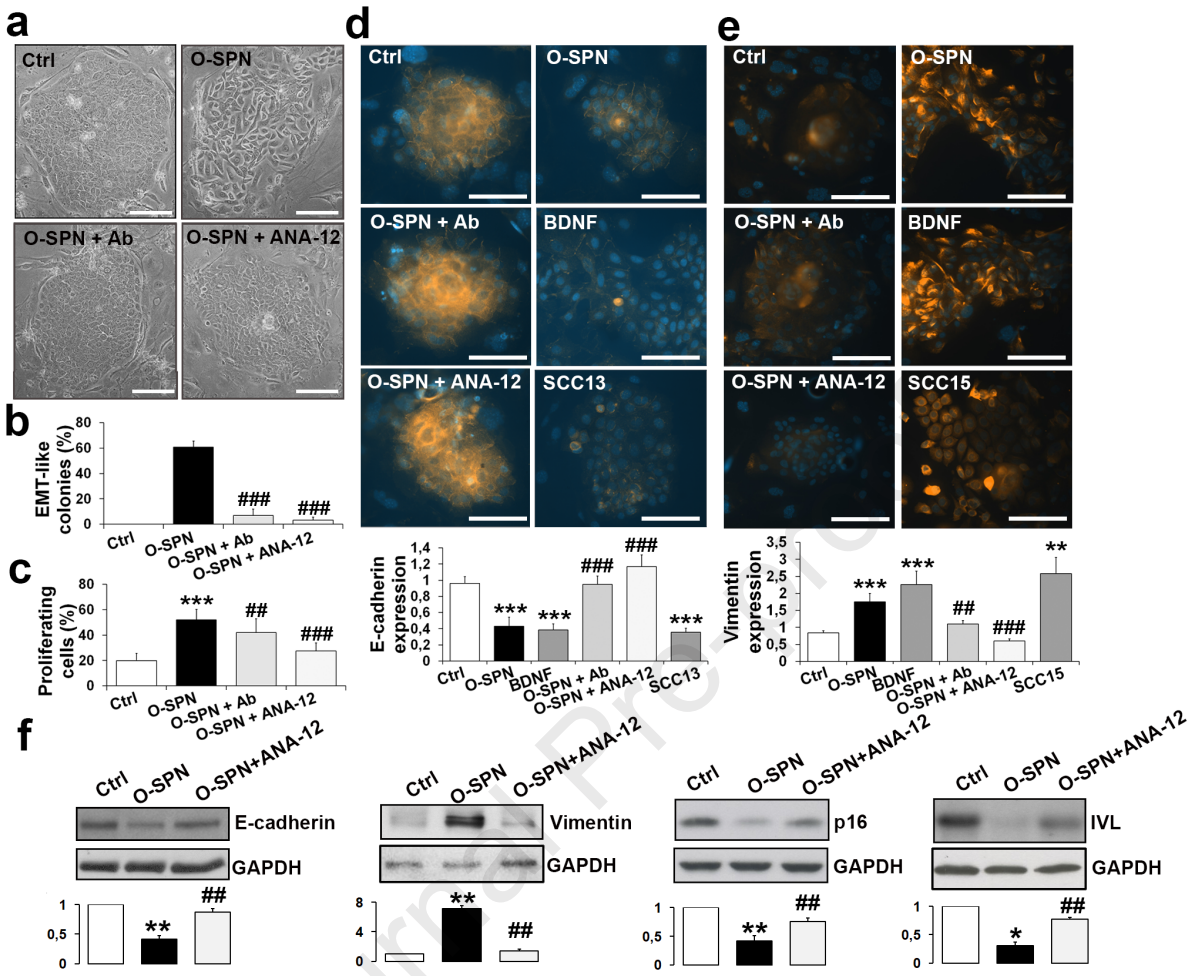

Figure 4

a

BDNF pathway	Ctrl		O-SPN		BDNF		O-SPN + ANA-12	
	Mean	±SD	Mean	±SD	Mean	±SD	Mean	±SD
AKT1	1,04	0,33	0,55	0,11	0,57	0,14	1,05	0,26
PIK3CA	1	0,1	1,8	0,51	1,7	0,35	0,99	0,18
GSK3B	1,09	0,54	1,88	0,32	1,9	0,16	1,04	0,52
TP53	1,04	0,35	0,54	0,21	0,53	0,12	0,82	0,46
STAT3	1,08	0,5	2,18	0,11	1,91	0,38	1,36	0,23
MAP2K1	1,04	0,34	1,94	0,51	2,25	0,36	1,15	0,27
MAPK14	1	0,1	1,32	0,39	1,17	0,07	0,9	0,12
EMT Trascription Factors (EMT master genes)	Ctrl		O-SPN		BDNF		O-SPN + ANA-12	
	Mean	±SD	Mean	±SD	Mean	±SD	Mean	±SD
SNAI1	1,01	0,19	2,33	0,45	1,83	0,24	1,13	0,59
TWIST1	1	0,03	2,61	0,09	8,96	0,49	1,27	0,14
ZEB1	1,01	0,18	3,25	1,48	4,87	1,59	1,44	0,11
ZEB2	0,95	0,33	2,06	0,45	2,41	0,79	0,93	0,52
Cell-matrix adhesion	Ctrl		O-SPN		BDNF		O-SPN + ANA-12	
	Mean	±SD	Mean	±SD	Mean	±SD	Mean	±SD
COL1A1	1,25	1,05	2,83	0,74	9,29	3,78	1,7	0,31
COL3A1	1,06	0,44	2,37	0,92	5,11	1,37	0,97	0,2
FN1	1,02	0,13	1,45	0,25	2,59	1,59	0,69	0,05
ITGB1	1	0,1	1,13	0,07	1,18	0,25	0,53	0,26
SERPINE1	1,09	0,54	1,41	0,36	1,93	1,83	0,87	0,1
Mesenchymal markers	Ctrl		O-SPN		BDNF		O-SPN + ANA-12	
	Mean	±SD	Mean	±SD	Mean	±SD	Mean	±SD
DDR1	1,17	0,44	2,2	0,22	1,7	0,26	0,83	0,01
THY1	1,01	0,15	1,88	0,31	6,43	3,31	1,3	0,55
VIM	1,01	0,18	1,55	0,12	1,4	0,26	0,89	0,05
Hippo pathway	Ctrl		O-SPN		BDNF		O-SPN + ANA-12	
	Mean	±SD	Mean	±SD	Mean	±SD	Mean	±SD
YAP1	1	0,11	2,25	0,28	1,7	0,06	1,75	0,3
TAZ	1,03	0,26	1,64	0,38	1,68	0,35	0,79	0,16
LATS1	1,01	0,2	1,14	0,09	1,16	0,31	0,58	0,34
WWC1	1	0,07	1,45	0,33	1,26	0,42	1,08	0,17
Notch pathway	Ctrl		O-SPN		BDNF		O-SPN + ANA-12	
	Mean	±SD	Mean	±SD	Mean	±SD	Mean	±SD
NOTCH1	1	0,01	0,4	0,26	0,58	0,13	0,61	0,23
DLL1	1,03	0,31	1,87	0,28	3,9	1,93	0,75	0,41
DLL4	1,01	0,18	0,6	0,01	0,42	0,02	1,45	0,12
JAG1	1,01	0,17	0,76	0,36	0,55	0,13	1,28	0,17
p<	0,001	0,01	0,05	ns	0,001	0,01	0,05	ns

b

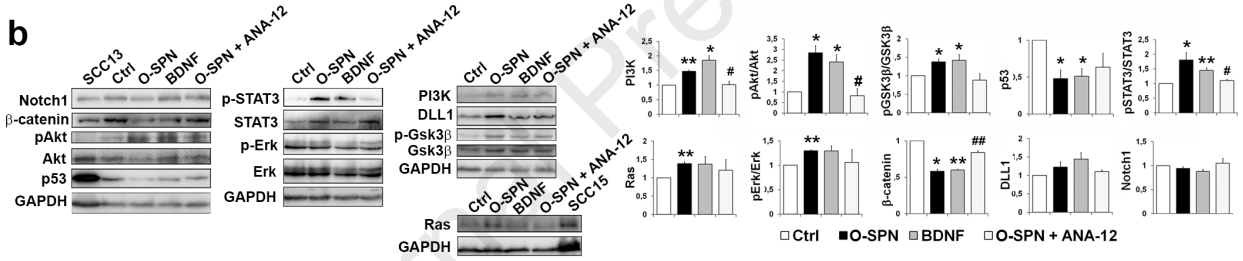

c

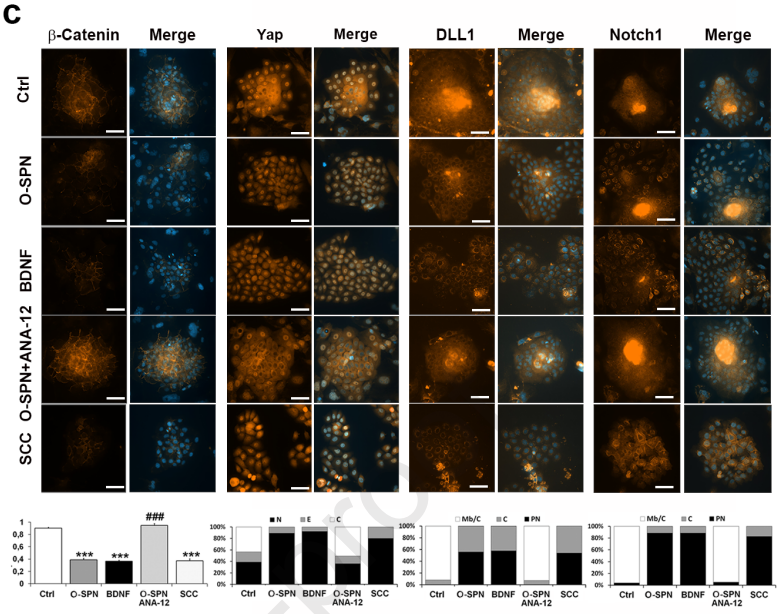

Figure 5

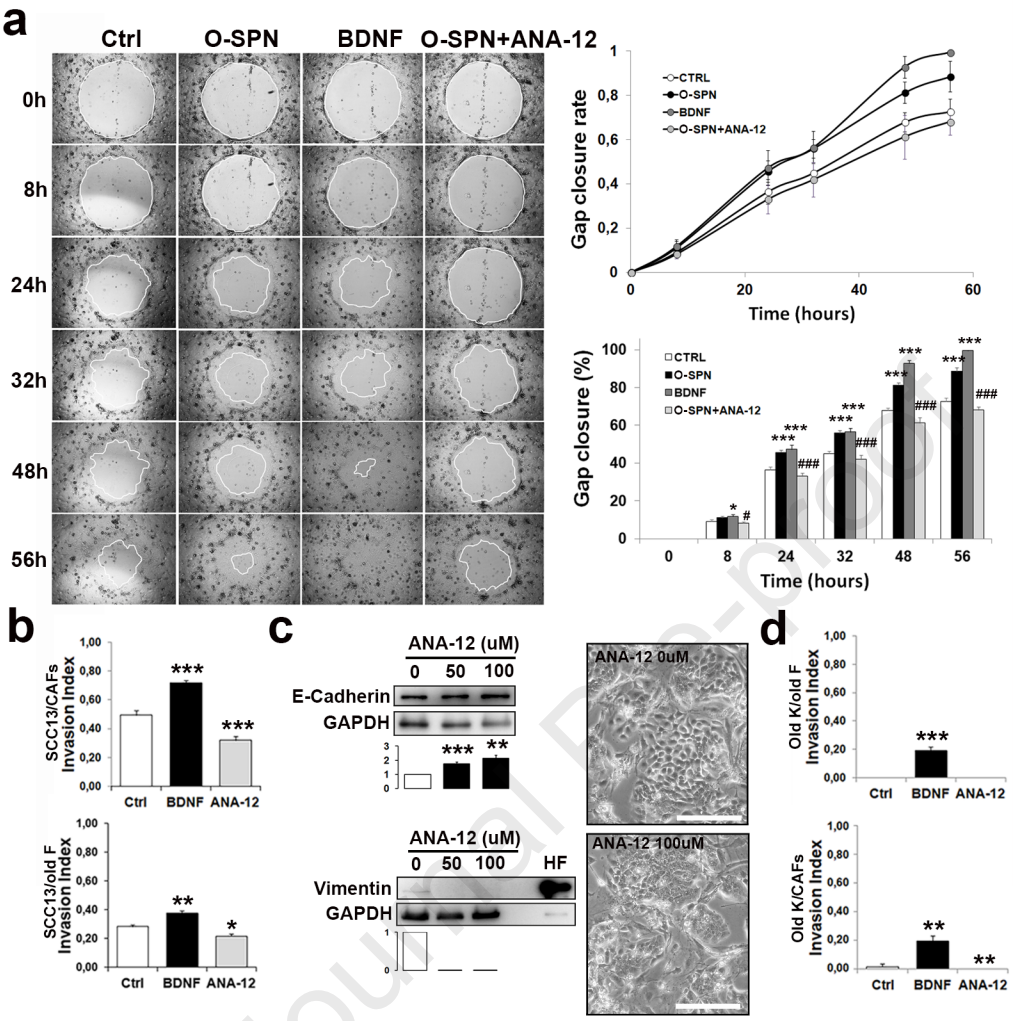

Table S1. Primer sequences for the genes assessed using qRT-PCR

mRNA	*Forward*	*Reverse*
p75	*5'ACGGCTACTACCAGGATGAG 3'*	*5' TGGCCTCGTCGGAATACGTG 3'*
TrkB-FL	*5' AGGAAATTCACGACGGAAAG 3'*	*5' TCACCTCATTGTTTGACAGC 3'*
TrkB.T1	*5' TCTATGCTGTGGTGGTGATTG 3'*	*5' GAGTCCAGCTTACATGGCAG 3'*
TrkB.T.Shc	*5' TTTGCTGTCCAGTGATCCCC 3'*	*5' ATAGAGGCCTCCTTGCCAGA 3'*
Snail	*5'GCTGCAGGACTCTAATCCAGA3'*	*5'ATCTCCGGAGGTGGGATG 3'*
Slug	*5'TGGTTGCTTCAAGGACACAT 3'*	*5'GTTGCAGTGAGGGCAAGAA 3'*
Twist	*5'GGAGTCCGCAGTCTTACGAG3'*	*5'CCAGCTTGAGGGTCTGAATC 3'*
Zeb1	*5'GGGAGGAGCAGTGAAAGAGA 3'*	*5'TTTCTTGCCCTTCCTTTCTG 3'.*
Zeb2	*5'AAGCCAGGGACAGATCAGC 3'*	*5'CCACACTCTGTGCATTTGAACT 3'*
GUSB	*5'TGCAGGTGATGGAAGAAGTG 3'*	*5' TTGCTCACAAAGGTCACAGG 3'*

Table S2. Antibodies for immunofluorescence and immunoblots

Antibody	Company	Catalog Number	Description	Immunoblot	Immunofluorescence
E-cadherin	BD Biosciences, San Jose, CA, USA	610181	Mouse monoclonal	1:2000	1:1000
β-catenin	Santa Cruz, Dallas, Texas, USA	sc-7963	Mouse monoclonal	1:500	1:200
Notch 1	abcam, Cambridge UK	65297	Mouse monoclonal	1:1000	1:200
DLL1	Santa Cruz, Dallas, Texas, USA	sc-377310	Mouse monoclonal	1:200	1:100
YAP	Santa Cruz, Dallas, Texas, USA	sc-101199	Mouse monoclonal	1:1000	1:200
p53	Santa Cruz, Dallas, Texas, USA	sc-126	Mouse monoclonal	1:500	
Phospho-Erk1/2	Cell Signaling, Danvers, MA, USA	9102S	Rabbit polyclonal	1:100	
Erk1/2	Cell Signaling, Danvers, MA, USA	9102S	Mouse monoclonal	1:1000	
Phospho-Akt	Cell Signaling, Danvers, MA, USA	9271S	Rabbit polyclonal	1:500	
Akt	Cell Signaling, Danvers, MA, USA	2920S	Mouse monoclonal	1:500	
PI3K	Cell Signaling, Danvers, MA, USA	4255S	Rabbit polyclonal	1:100	
Phospho-GSK-3β	Santa Cruz, Dallas, Texas, USA	sc-373800	Rabbit polyclonal	1:100	
GSK-3β	Santa Cruz, Dallas, Texas, USA	sc-377213	Mouse monoclonal	1:1000	
Phospho-STAT3	Cell Signaling, Danvers, MA, USA	9131S	Rabbit polyclonal	1:500	
STAT3	Santa Cruz, Dallas, Texas, USA	sc-8019	Mouse monoclonal	1:1000	
p21 Ras	BD Biosciences, San Jose, CA, USA	610001	Mouse monoclonal	1:500	
P21 Waf	A gift from Kristian Helin (IEO, Milan, Italy).	-	Mouse monoclonal	1:3	
PCNA	Santa Cruz, Dallas, Texas, USA	sc-56	Mouse monoclonal	1:1000	
Bmi-1	Merk Life Science S.r.l., Italy	05-637	Mouse monoclonal	1:100	
P63	Santa Cruz, Dallas, Texas, USA	sc-8431	Mouse monoclonal	1:100	

Vimentin	BD Biosciences, San Jose, CA, USA	550513	Mouse monoclonal	1:5000	1:1000
Involucrin	Sigma-Aldrich, St. Louis, MO, USA	I9018	Mouse monoclonal	1:1000	
p16	BD Biosciences, San Jose, CA, USA	550834	Mouse monoclonal	1:100	
α-Smooth Muscle	Sigma-Aldrich, St. Louis, MO, USA	A2547	Mouse monoclonal	1:1000	
BDNF	Sigma-Aldrich, St. Louis, MO, USA	SAB1402127 -100UG	Mouse monoclonal	1:100	
Serpin E1/PAI-1	R&D Systems, Minneapolis, MN, USA	MAB1786	Mouse monoclonal	1:100	
GAPDH	Santa Cruz, Dallas, Texas, USA	FL-335	Rabbit polyclonal	1:1000	
HRP-Anti-mouse	GE Healthcare UK Limited, Little Chalfont Buckinghamshire	NA931V		1:5000	
HRP-Anti-rabbit	GE Healthcare UK Limited, Little Chalfont Buckinghamshire	NA934VS		1:5000	
Biotinylated-Anti-mouse	Vector Laboratories, Inc. Burlingame, CA, USA	BA-2000			1:200
Biotinylated-Anti-rabbit	Vector Laboratories, Inc. Burlingame, CA, USA	BA-1000			1:200
Alexa Fluor™ 555 conjugate Streptavidin	Thermo Fischer Scientific, Waltham, MA, USA	S21381			1:500
Anti-rabbit Alexa Fluor® 488 conjugate	Thermo Fischer Scientific, Waltham, MA, USA	A21206			1:200

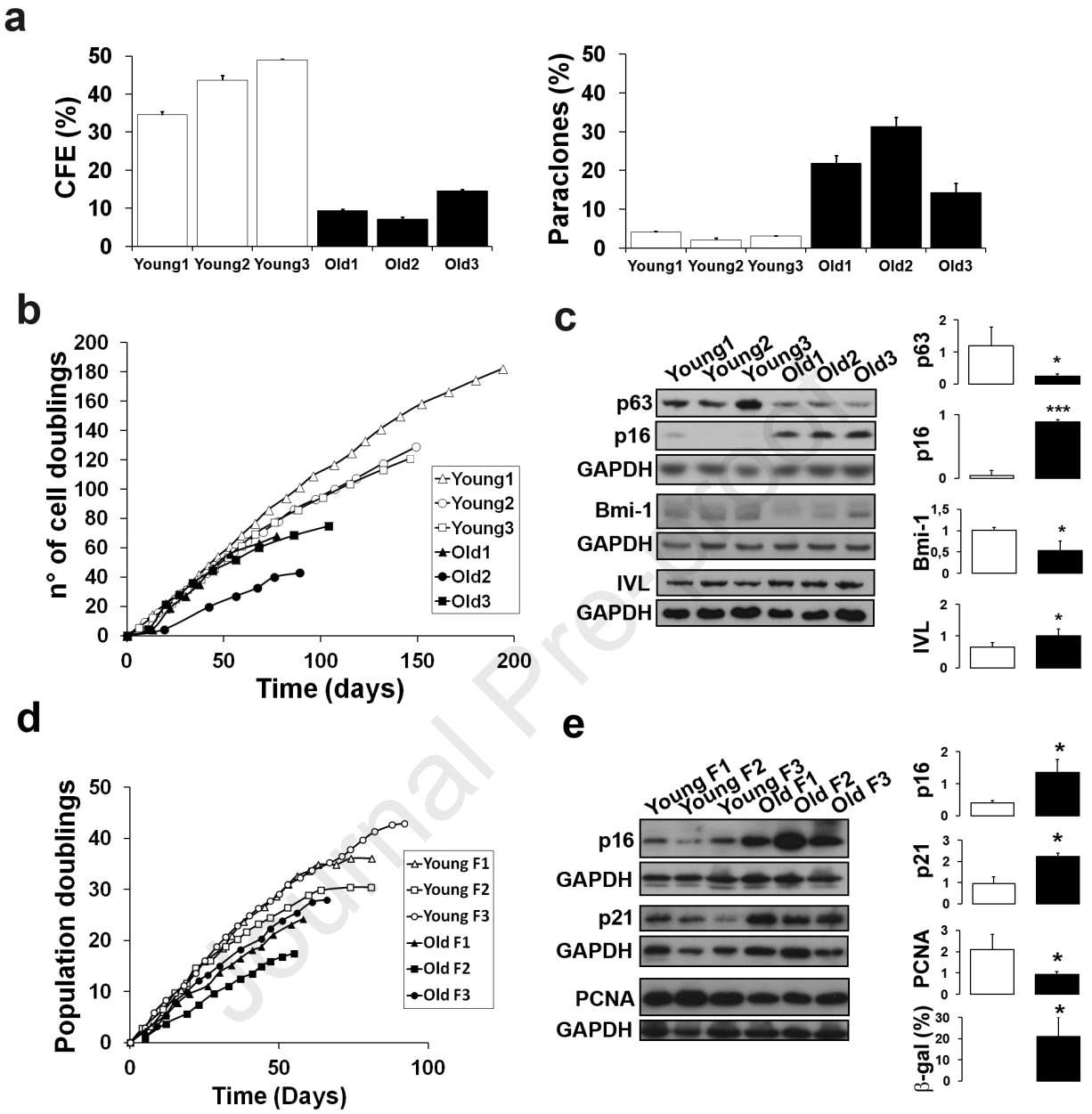
a
CFE (%)
Young1 Young2 Young3 Old1 Old2 Old3
Paraclones (%)
Young1 Young2 Young3 Old1 Old2 Old3
b
n° of cell doublings
Time (days)
Young1
Young2
Young3
Old1
Old2
Old3
c
Young1 Young2 Young3 Old1 Old2 Old3
p63
p16
GAPDH
Bmi-1
GAPDH
IVL
GAPDH
d
Population doublings
Time (Days)
Young F1
Young F2
Young F3
Old F1
Old F2
Old F3
e
Young F1 Young F2 Young F3 Old F1 Old F2 Old F3
p16
GAPDH
p21
GAPDH
PCNA
GAPDH
β-gal (%)

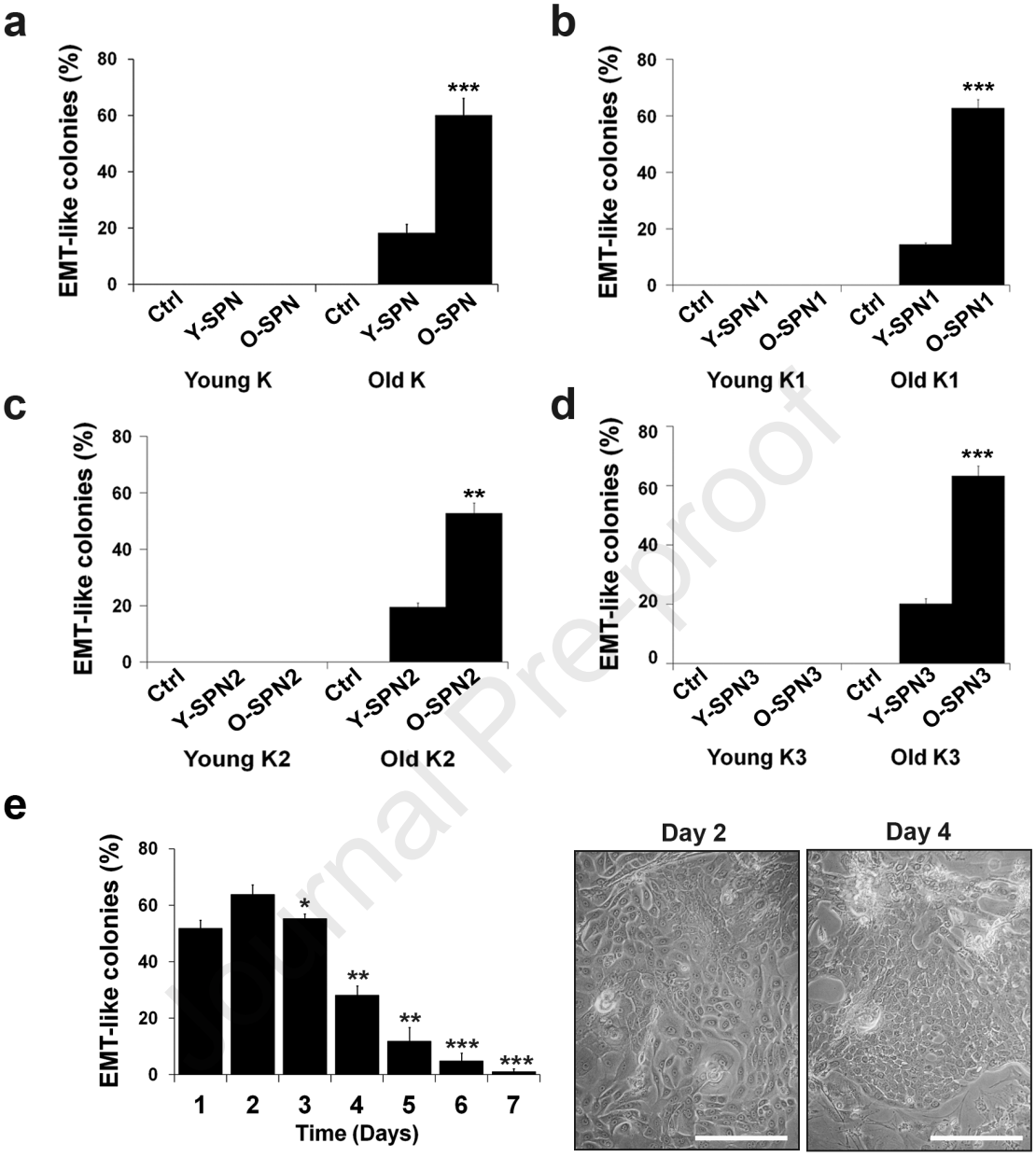

a

Protein	*Y-SPN*	*O-SPN*	*p*
BDNF	0.21±0.19	4.95±1.05	0.0001
CCL2	60.88±44.78	6.34±3.11	0.031
FGF9	0.04±0.03	1.30±1.13	0.04
IL12B	-	0.77±0.41	0.01
M CSF (OSM)	0.05±0.05	0.54±0.44	0.04
MMP3	3.65±1.51	6.81±0.97	0.002
TIMP1	6.95±1.03	3.91±1.05	0.001
TIMP2	7.20±1.61	3.61±1.26	0.002
TIMP4	0.37±0.05	0.17±0.18	0.04
TNFSF11B	0.41±0.46	2.70±1.78	0.02
TNFSF14	0.18±0.10	0.66±0.34	0.02

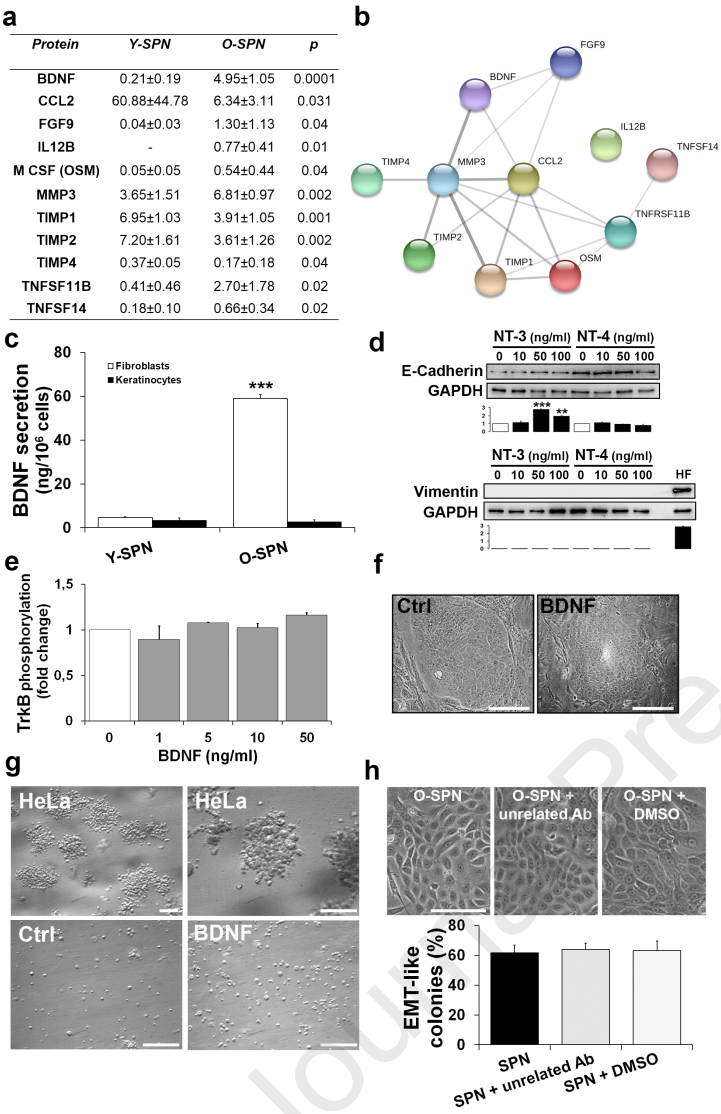

	Ctrl		O-SPN			BDNF			O-SPN + ANA-12		
	Media	*SD*	*Media*	*SD*	*ttest*	*Media*	*SD*	*ttest*	*Media*	*SD*	*ttest*
ABCB5	1,06	0,42	0,32	0,01	0,05	0,26	0,05	0,04	0,77	0,06	0,003
ABCG2	1,06	0,24	0,67	0,28	0,17	1,02	0,18	0,45	0,95	0,14	0,22
ABL1	1,12	0,38	1,13	0,15	0,49	1,28	0,15	0,36	1,30	0,38	0,35
AKT1	1,04	0,33	0,55	0,11	0,05	0,57	0,14	0,05	1,05	0,26	0,03
ALCAM	1,05	0,23	1,65	0,38	0,13	1,94	0,46	0,09	1,94	0,19	0,27
ALDH1A1	1,11	0,34	0,33	0,24	0,07	0,30	0,09	0,07	0,52	0,11	0,26
ALDH1A3	1,07	0,30	0,58	0,14	0,12	1,07	0,18	0,49	0,88	0,22	0,16
ATM	1,00	0,03	1,50	0,03	0,0002	2,27	0,14	0,005	2,23	1,10	0,29
ATXN1	1,00	0,05	0,86	0,02	0,05	0,71	0,10	0,04	0,69	0,05	0,03
AXL	1,14	0,37	0,75	0,05	0,20	1,15	0,02	0,50	1,12	0,22	0,12
BMI1	1,00	0,05	1,03	0,15	0,43	0,92	0,04	0,13	1,21	0,29	0,31
BMP7	1,02	0,13	5,16	2,03	0,09	3,43	2,52	0,22	3,89	2,66	0,36
CALR	1,01	0,08	1,07	0,07	0,28	0,89	0,10	0,21	0,93	0,09	0,14
CCNA2	1,05	0,25	1,00	0,13	0,43	0,33	0,08	0,05	0,68	0,20	0,14
CCNB1	1,07	0,25	1,26	0,27	0,31	1,18	0,27	0,39	1,17	0,33	0,42
CCND1	1,00	0,06	0,85	0,02	0,05	1,13	0,30	0,36	0,88	0,15	0,43
CCNE1	1,01	0,10	0,73	0,04	0,05	0,55	0,03	0,02	0,63	0,10	0,21
CD24	1,00	0,06	1,46	0,17	0,05	2,31	0,41	0,04	1,99	0,34	0,13
CD34	1,01	0,11	0,59	0,01	0,03	0,47	0,06	0,01	1,11	0,33	0,13
CD38	1,00	0,10	0,20	0,04	0,001	0,19	0,04	0,001	0,44	0,25	0,11
CD44	1,03	0,28	1,43	0,44	0,13	1,59	0,65	0,13	0,72	0,05	0,05
CDC25C	1,09	0,28	1,38	0,00	0,21	1,99	0,28	0,05	1,46	0,51	0,44
CDK2	1,04	0,21	1,06	0,12	0,48	0,80	0,17	0,21	0,81	0,13	0,12
CDK4	1,04	0,20	1,41	0,44	0,25	0,99	0,12	0,42	0,87	0,06	0,17
CDK6	1,00	0,06	0,66	0,23	0,05	1,00	0,31	0,49	0,85	0,12	0,14
CDKN1A	1,01	0,09	1,20	0,05	0,07	0,52	0,04	0,01	1,10	0,29	0,39
CDKN1B	1,07	0,28	0,89	0,16	0,30	0,64	0,19	0,14	0,85	0,15	0,44
CDKN1C	1,09	0,55	0,74	0,57	0,25	0,18	0,09	0,05	1,04	0,96	0,34
CDKN2A	1,00	0,07	0,81	0,26	0,27	0,73	0,17	0,12	0,84	0,06	0,45
CDKN2B	1,04	0,20	0,67	0,04	0,11	1,68	0,67	0,22	0,72	0,05	0,24
CDKN2C	1,03	0,17	0,97	0,33	0,44	0,85	0,13	0,23	0,53	0,03	0,15
CDKN2D	1,05	0,37	1,27	0,08	0,20	1,60	0,19	0,05	0,80	0,18	0,01
CHEK1	1,03	0,17	0,89	0,01	0,24	0,73	0,10	0,11	0,74	0,06	0,07
CHEK2	1,02	0,13	0,72	0,10	0,07	0,58	0,11	0,03	0,53	0,10	0,13
CITED2	1,07	0,43	1,38	0,29	0,18	2,65	0,12	0,01	1,10	0,17	0,12
COL1A1	1,25	1,05	2,83	0,74	0,05	9,29	3,78	0,03	1,70	0,31	0,05
COL3A1	1,06	0,44	2,37	0,92	0,05	5,11	1,37	0,01	0,97	0,20	0,05
CREG1	1,11	0,33	0,83	0,14	0,25	1,40	0,26	0,26	0,81	0,14	0,46
DACH1	1,08	0,30	1,62	0,31	0,14	0,39	0,03	0,07	1,78	0,48	0,40
DDR1	1,17	0,44	2,20	0,22	0,06	1,70	0,26	0,19	0,83	0,01	0,01
DKK1	1,01	0,09	1,35	0,30	0,18	2,67	0,25	0,01	1,49	0,13	0,36
DLL1	1,03	0,31	1,87	0,28	0,01	3,90	1,93	0,05	0,75	0,41	0,01
DLL4	1,01	0,18	0,60	0,01	0,03	0,42	0,02	0,01	1,45	0,12	0,003
DNMT1	1,05	0,22	0,77	0,14	0,18	0,61	0,17	0,10	1,02	0,13	0,13
E2F1	1,07	0,26	1,14	0,18	0,42	0,95	0,27	0,38	0,67	0,13	0,06
E2F3	1,28	0,59	0,48	0,00	0,15	1,45	0,16	0,40	0,97	0,44	0,19
EGF	1,01	0,11	0,50	0,11	0,01	0,51	0,03	0,02	0,15	0,03	0,04
EGR1	1,00	0,10	0,72	0,30	0,12	0,47	0,21	0,01	0,79	0,02	0,36
ENG	1,00	0,05	0,56	0,17	0,05	3,25	2,37	0,22	0,33	0,02	0,15
EPCAM	1,00	0,03	0,94	0,17	0,37	1,01	0,28	0,48	1,50	0,17	0,04
ERBB2	1,00	0,05	2,10	0,41	0,06	0,74	0,23	0,19	1,52	0,28	0,16
ETFA	1,01	0,18	0,51	0,29	0,04	0,33	0,13	0,004	0,81	0,12	0,10
ETS1	1,01	0,08	1,08	0,09	0,29	1,08	0,07	0,26	0,89	0,03	0,09
ETS2	1,02	0,14	0,79	0,06	0,12	0,58	0,12	0,04	0,79	0,02	0,48
FGFR2	1,00	0,02	0,84	0,22	0,27	0,87	0,16	0,26	1,04	0,37	0,33
FLOT2	1,03	0,32	0,68	0,10	0,10	0,91	0,34	0,34	1,18	0,34	0,06
FN1	1,02	0,13	1,45	0,25	0,11	2,59	1,59	0,21	0,69	0,05	0,04
FOXA2	1,01	0,18	0,89	0,27	0,27	0,47	0,10	0,01	1,83	0,52	0,03
FOXP1	1,03	0,17	0,88	0,23	0,32	0,73	0,27	0,21	0,93	0,14	0,44
FZD7	1,03	0,18	0,66	0,19	0,11	0,96	0,04	0,36	0,73	0,07	0,37
GADD45A	1,00	0,05	0,88	0,08	0,13	0,98	0,09	0,43	0,59	0,10	0,04
GATA3	1,00	0,04	0,80	0,17	0,18	0,78	0,16	0,14	0,51	0,08	0,12
GLB1	1,22	0,92	2,26	0,62	0,09	3,46	1,20	0,03	0,97	0,29	0,03
GSK3B	1,09	0,54	1,88	0,32	0,05	1,90	0,16	0,05	1,04	0,52	0,04
HDAC1	1,02	0,13	0,74	0,05	0,08	0,90	0,05	0,23	0,83	0,04	0,12
HRAS	1,03	0,17	0,90	0,27	0,35	0,93	0,31	0,40	0,71	0,10	0,28
ID1	1,00	0,05	0,85	0,18	0,25	0,69	0,29	0,20	1,15	0,17	0,15
IFNG	1,21	0,52	1,17	0,47	0,48	0,31	0,02	0,11	0,62	0,03	0,25
IGF1	1,05	0,22	0,18	0,01	0,03	2,85	0,75	0,06	0,15	0,00	0,06
IGF1R	1,08	0,28	1,27	0,12	0,29	1,40	0,21	0,20	0,94	0,23	0,14
IGFBP3	1,03	0,19	0,70	0,20	0,15	5,07	0,22	0,00	0,37	0,07	0,12
IGFBP5	1,05	0,23	0,47	0,19	0,07	1,59	0,48	0,20	0,36	0,03	0,31
IGFBP7	1,01	0,14	0,45	0,12	0,003	0,40	0,15	0,004	0,54	0,17	0,25
IKBKB	1,00	0,06	1,14	0,24	0,32	0,87	0,14	0,23	1,18	0,05	0,44
IL8	1,00	0,05	2,17	0,08	0,00	0,43	0,15	0,02	1,58	0,09	0,00
ING1	1,05	0,40	1,27	0,09	0,22	2,02	0,50	0,03	0,83	0,01	0,01
IRF3	1,04	0,21	1,30	0,13	0,18	0,56	0,05	0,07	0,88	0,13	0,04
IRF5	1,00	0,05	0,63	0,32	0,18	1,90	0,22	0,02	0,79	0,11	0,34
IRF7	1,00	0,06	1,54	0,41	0,16	2,16	0,83	0,15	0,65	0,11	0,08

	Ctrl		O-SPN			BDNF			O-SPN + ANA-12		
	Media	*SD*	*Media*	*SD*	*ttest*	*Media*	*SD*	*ttest*	*Media*	*SD*	*ttest*
ITGA2	1,00	0,02	0,59	0,07	0,01	0,80	0,10	0,09	0,58	0,11	0,46
ITGA4	1,00	0,06	0,56	0,22	0,03	0,79	0,40	0,23	0,72	0,25	0,22
ITGA6	1,00	0,07	0,97	0,13	0,42	1,18	0,10	0,12	0,65	0,11	0,07
ITGB1	1,00	0,10	1,13	0,07	0,09	1,18	0,25	0,17	0,53	0,26	0,02
JAG1	1,01	0,17	0,76	0,36	0,18	0,55	0,13	0,01	1,28	0,17	0,05
JAK2	1,01	0,08	1,03	0,01	0,41	0,83	0,25	0,28	0,58	0,15	0,05
KIT	1,66	1,84	0,24	0,06	0,16	0,37	0,24	0,17	0,74	0,30	0,05
KITLG	1,01	0,09	0,86	0,09	0,16	0,96	0,11	0,38	0,99	0,01	0,14
KLF17	1,02	0,15	1,73	0,59	0,18	2,12	0,45	0,06	1,57	0,07	0,41
KLF4	1,04	0,20	1,39	0,36	0,23	1,12	0,05	0,37	0,79	0,14	0,12
LATS1	1,01	0,20	1,14	0,09	0,20	1,16	0,31	0,26	0,58	0,34	0,05
LIN28A	1,01	0,19	1,15	0,92	0,41	3,48	1,09	0,03	0,78	0,54	0,29
LIN28B	1,01	0,18	0,60	0,01	0,03	0,48	0,11	0,01	1,46	0,12	0,003
MAML1	1,05	0,21	0,46	0,12	0,05	15,53	1,53	0,005	0,96	0,22	0,07
MAP2K1	1,04	0,34	1,94	0,51	0,04	2,25	0,36	0,01	1,15	0,27	0,05
MAP2K3	1,03	0,17	0,80	0,08	0,16	0,50	0,06	0,04	0,70	0,13	0,29
MAP2K6	1,05	0,22	0,31	0,01	0,04	0,49	0,23	0,08	0,15	0,02	0,01
MAPK14	1,00	0,10	1,32	0,39	0,15	1,17	0,07	0,04	0,90	0,12	0,10
MDM2	1,10	0,35	0,94	0,07	0,35	1,08	0,24	0,48	0,83	0,20	0,31
MERTK	1,10	0,34	0,74	0,43	0,27	0,58	0,16	0,13	0,51	0,02	0,32
MORC3	1,02	0,15	1,01	0,27	0,48	0,97	0,08	0,38	0,68	0,04	0,18
MS4A1	1,01	0,18	0,59	0,01	0,03	0,47	0,10	0,01	1,44	0,11	0,003
MUC1	1,00	0,10	1,75	0,56	0,07	1,62	0,05	0,001	1,58	0,54	0,36
MYC	1,00	0,07	1,20	0,13	0,14	1,04	0,12	0,41	0,91	0,12	0,09
MYCN	1,06	0,23	0,87	0,18	0,28	2,28	0,12	0,01	0,74	0,29	0,37
NANOG	1,04	0,20	0,85	0,13	0,24	1,68	0,38	0,11	0,59	0,13	0,12
NBN	1,16	0,38	0,60	0,08	0,14	0,52	0,03	0,12	0,58	0,16	0,46
NFKB1	1,01	0,20	1,04	0,03	0,41	0,84	0,13	0,14	1,36	0,16	0,03
NOS2	1,01	0,19	0,62	0,05	0,03	0,60	0,20	0,03	1,48	0,12	0,001
NOTCH1	1,00	0,01	0,40	0,26	0,03	0,58	0,13	0,02	0,61	0,23	0,18
NOTCH2	1,00	0,03	1,21	0,24	0,24	0,54	0,10	0,02	0,77	0,09	0,10
NOX4	1,13	0,39	1,25	0,36	0,42	0,36	0,01	0,09	0,56	0,11	0,09
PCNA	1,02	0,14	1,27	0,06	0,10	0,87	0,15	0,25	0,74	0,14	0,02
PECAM1	1,01	0,18	0,60	0,01	0,03	0,48	0,11	0,01	1,47	0,12	0,003
PIK3CA	1,00	0,10	1,80	0,51	0,05	1,70	0,35	0,03	0,99	0,18	0,05
PLAT	1,18	0,45	1,36	0,09	0,36	0,75	0,12	0,22	2,41	2,00	0,33
PLAU	1,03	0,17	0,73	0,02	0,11	1,61	0,42	0,15	0,95	0,17	0,16
PLAUR	1,03	0,28	0,74	0,29	0,14	0,49	0,18	0,03	1,24	0,48	0,11
POU5F1	1,04	0,35	1,91	0,55	0,05	4,24	0,14	0,001	0,83	0,16	0,03
PRKCD	1,00	0,04	1,27	0,27	0,22	0,82	0,26	0,28	0,63	0,08	0,07
PROM1	1,05	0,38	0,45	0,07	0,05	0,41	0,04	0,05	0,71	0,39	0,19
PTCH1	1,01	0,21	1,41	0,15	0,03	2,41	0,53	0,01	0,42	0,24	0,003
PTEN	1,01	0,09	0,93	0,18	0,35	1,21	0,11	0,11	0,77	0,01	0,24
PTPRC	1,01	0,18	0,59	0,01	0,03	0,47	0,10	0,01	1,40	0,13	0,004
RB1	1,01	0,08	0,65	0,14	0,05	0,43	0,08	0,00	0,55	0,13	0,30
RBL1	1,01	0,09	0,97	0,05	0,37	0,55	0,20	0,07	0,52	0,07	0,00
RBL2	1,04	0,21	0,77	0,05	0,16	0,74	0,19	0,17	0,63	0,13	0,20
SAB1	1,02	0,14	1,20	0,13	0,20	1,40	0,23	0,12	1,37	0,16	0,23
SERPINB2	1,04	0,20	0,96	0,12	0,38	1,03	0,49	0,49	0,82	0,15	0,26
SERPINE1	1,09	0,54	1,41	0,36	0,22	1,93	1,83	0,26	0,87	0,10	0,05
SIRT1	1,00	0,04	0,80	0,18	0,19	0,73	0,08	0,03	0,69	0,06	0,30
SMO	1,01	0,09	0,68	0,40	0,25	1,01	0,16	0,49	1,42	0,06	0,10
SNAI1	1,01	0,19	2,33	0,45	0,01	1,83	0,24	0,01	1,13	0,59	0,03
SOD1	1,06	0,25	0,59	0,06	0,10	0,50	0,06	0,07	0,60	0,11	0,47
SOD2	1,00	0,02	1,02	0,05	0,40	0,99	0,28	0,48	0,71	0,03	0,00
SOX2	1,01	0,18	0,59	0,01	0,03	0,55	0,14	0,01	1,44	0,11	0,003
SPARC	1,01	0,08	0,67	0,13	0,05	2,36	1,48	0,23	0,77	0,17	0,33
STAT3	1,08	0,50	2,18	0,11	0,03	1,91	0,38	0,04	1,36	0,23	0,01
TAZ	1,03	0,26	1,64	0,38	0,04	1,68	0,35	0,03	0,79	0,16	0,02
TBX2	1,06	0,27	1,09	0,31	0,48	0,33	0,02	0,06	0,59	0,03	0,12
TBX3	1,04	0,21	1,67	0,48	0,16	1,29	0,26	0,25	0,88	0,32	0,13
TERF2	1,01	0,20	0,58	0,19	0,02	0,60	0,13	0,02	0,75	0,20	0,17
TERT	1,28	0,63	1,22	0,41	0,47	0,31	0,01	0,13	0,58	0,03	0,13
TGFB1	1,05	0,42	0,43	0,12	0,05	0,82	0,04	0,22	2,29	0,89	0,03
TGFBR1	1,06	0,43	0,92	0,16	0,33	1,96	0,19	0,03	0,76	0,09	0,11
TGFB1I1	1,01	0,09	1,02	0,02	0,46	1,43	0,25	0,11	0,96	0,09	0,31
THBS1	1,00	0,05	0,78	0,13	0,12	2,32	1,02	0,16	0,79	0,15	0,48
THY1	1,01	0,15	1,88	0,31	0,01	6,43	3,31	0,05	1,30	0,55	0,11
TP53	1,04	0,35	0,54	0,21	0,05	0,53	0,12	0,05	0,82	0,46	0,29
TP53BP1	1,01	0,10	0,85	0,08	0,14	0,96	0,15	0,40	0,86	0,10	0,47
TWIST1	1,00	0,03	2,61	0,09	0,0001	8,96	0,49	0,001	1,27	0,14	0,0001
TWIST3	1,07	0,24	0,78	0,23	0,22	0,35	0,11	0,04	0,35	0,01	0,10
VIM	1,01	0,18	1,55	0,12	0,01	1,40	0,26	0,05	0,89	0,05	0,003
WEE1	1,06	0,56	3,24	0,95	0,02	2,61	1,57	0,11	1,32	0,30	0,03
WNT1	1,01	0,18	0,57	0,05	0,02	0,47	0,10	0,01	1,44	0,11	0,001
WWC1	1,00	0,07	1,45	0,33	0,15	1,26	0,42	0,30	1,08	0,17	0,19
YAP1	1,00	0,11	2,25	0,28	0,004	1,70	0,06	0,001	1,75	0,30	0,05
ZEB1	1,01	0,18	3,25	1,48	0,05	4,87	1,59	0,03	1,44	0,11	0,08
ZEB2	0,95	0,33	2,06	0,45	0,01	2,41	0,79	0,03	0,93	0,52	0,02

A

	Control		O-SPN		BDNF		O-SPN + ANA-12	
	Media	*SD*	*Media*	*SD*	*Media*	*SD*	*Media*	*SD*
ABCB5	1,06	0,42	0,32	0,01	0,26	0,05	0,77	0,06
AKT1	1,04	0,33	0,55	0,11	0,57	0,14	1,05	0,26
CD38	1,00	0,10	0,20	0,04	0,19	0,04	0,44	0,25
CDK6	1,00	0,06	0,66	0,23	1,00	0,31	0,85	0,12
CDKN1C	1,09	0,55	0,74	0,57	0,18	0,09	1,04	0,96
DLL4	1,01	0,18	0,60	0,01	0,42	0,02	1,45	0,12
EGR1	1,00	0,10	0,72	0,30	0,47	0,21	0,79	0,02
ETFA	1,01	0,18	0,51	0,29	0,33	0,13	0,81	0,12
FOXA2	1,01	0,18	0,89	0,27	0,47	0,10	1,83	0,52
IGFBP7	1,01	0,14	0,45	0,12	0,40	0,15	0,54	0,17
ITGA4	1,00	0,06	0,56	0,22	0,79	0,40	0,72	0,25
JAG1	1,01	0,17	0,76	0,36	0,55	0,13	1,28	0,17
KIT	1,66	1,84	0,24	0,06	0,37	0,24	0,74	0,30
LIN28B	1,01	0,18	0,60	0,01	0,48	0,11	1,46	0,12
MS4A1	1,01	0,18	0,59	0,01	0,47	0,10	1,44	0,11
NFKB1	1,01	0,20	1,04	0,03	0,84	0,13	1,36	0,16
NOS2	1,01	0,19	0,62	0,05	0,60	0,20	1,48	0,12
NOTCH1	1,00	0,01	0,40	0,26	0,58	0,13	0,61	0,23
PECAM1	1,01	0,18	0,60	0,01	0,48	0,11	1,47	0,12
PLAUR	1,03	0,28	0,74	0,29	0,49	0,18	1,24	0,48
PROM1	1,05	0,38	0,45	0,07	0,41	0,04	0,71	0,39
PTPRC	1,01	0,18	0,59	0,01	0,47	0,10	1,40	0,13
SOX2	1,01	0,18	0,59	0,01	0,55	0,14	1,44	0,11
TERF2	1,01	0,20	0,58	0,19	0,60	0,13	0,75	0,20
TGFB1	1,05	0,42	0,43	0,12	0,82	0,04	2,29	0,89
TP53	1,04	0,35	0,54	0,21	0,53	0,12	0,82	0,46
WNT1	1,01	0,18	0,57	0,05	0,47	0,10	1,44	0,11
CD44	1,03	0,28	1,43	0,44	1,59	0,65	0,72	0,05
CDKN2D	1,05	0,37	1,27	0,08	1,60	0,19	0,80	0,18
CITED2	1,07	0,43	1,38	0,29	2,65	0,12	1,10	0,17
COL1A1	1,25	1,05	2,83	0,74	9,29	3,78	1,70	0,31
COL3A1	1,06	0,44	2,37	0,92	5,11	1,37	0,97	0,20
DDR1	1,17	0,44	2,20	0,22	1,70	0,26	0,83	0,01
DLL1	1,03	0,31	1,87	0,28	3,90	1,93	0,75	0,41
FN1	1,02	0,13	1,45	0,25	2,59	1,59	0,69	0,05
GLB1	1,22	0,92	2,26	0,62	3,46	1,20	0,97	0,29
GSK3B	1,09	0,54	1,88	0,32	1,90	0,16	1,04	0,52
ING1	1,05	0,40	1,27	0,09	2,02	0,50	0,83	0,01
ITGB1	1,00	0,10	1,13	0,07	1,18	0,25	0,53	0,26
LATS1	1,01	0,20	1,14	0,09	1,16	0,31	0,58	0,34
LIN28A	1,01	0,19	1,15	0,92	3,48	1,09	0,78	0,54
MAP2K1	1,04	0,34	1,94	0,51	2,25	0,36	1,15	0,27
MAPK14	1,00	0,10	1,32	0,39	1,17	0,07	0,90	0,12
MUC1	1,00	0,10	1,75	0,56	1,62	0,05	1,58	0,54
PIK3CA	1,00	0,10	1,80	0,51	1,70	0,35	0,99	0,18
POU5F1	1,04	0,35	1,91	0,55	4,24	0,14	0,83	0,16
PTCH1	1,01	0,21	1,41	0,15	2,41	0,53	0,42	0,24
SERPINE1	1,09	0,54	1,41	0,36	1,93	1,83	0,87	0,10
SNAI1	1,01	0,19	2,33	0,45	1,83	0,24	1,13	0,59
STAT3	1,08	0,50	2,18	0,11	1,91	0,38	1,36	0,23
TAZ	1,03	0,26	1,64	0,38	1,68	0,35	0,79	0,16
THY1	1,01	0,15	1,88	0,31	6,43	3,31	1,30	0,55
TWIST1	1,00	0,03	2,61	0,09	8,96	0,49	1,27	0,14
VIM	1,01	0,18	1,55	0,12	1,40	0,26	0,89	0,05
WEE1	1,06	0,56	3,24	0,95	2,61	1,57	1,32	0,30
YAP1	1,00	0,11	2,25	0,28	1,70	0,06	1,75	0,30
ZEB1	1,01	0,18	3,25	1,48	4,87	1,59	1,44	0,11
ZEB2	0,95	0,33	2,06	0,45	2,41	0,79	0,93	0,52

Legend p<	0,001	0,01	0,05	ns	0,001	0,01	0,05	ns

B

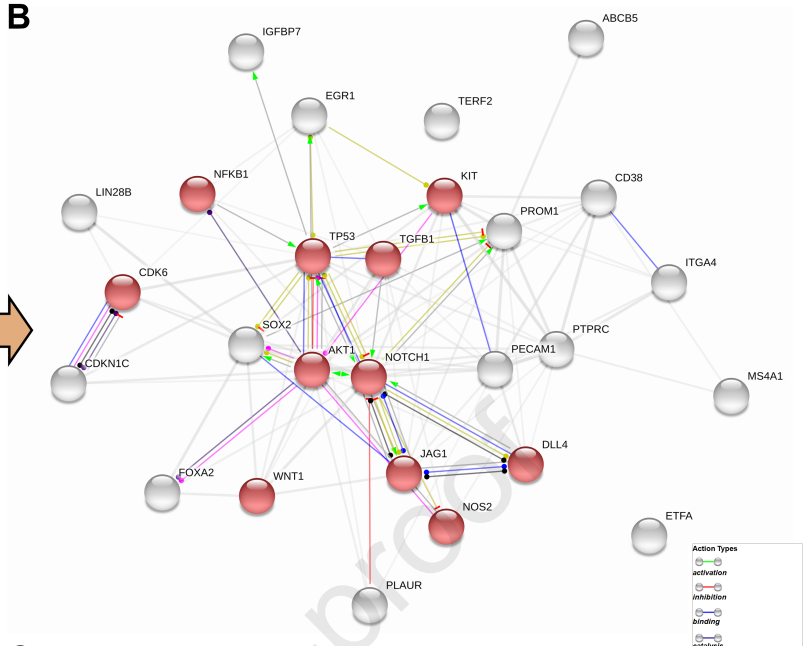

C

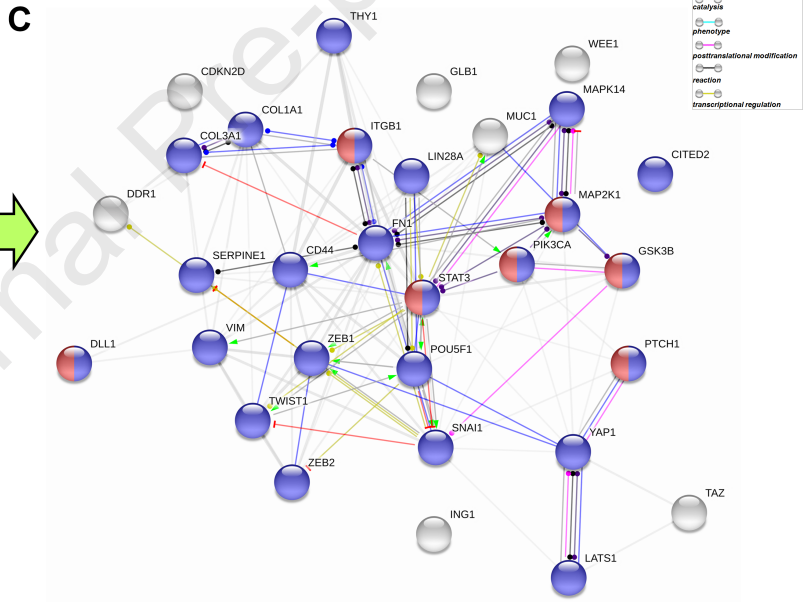

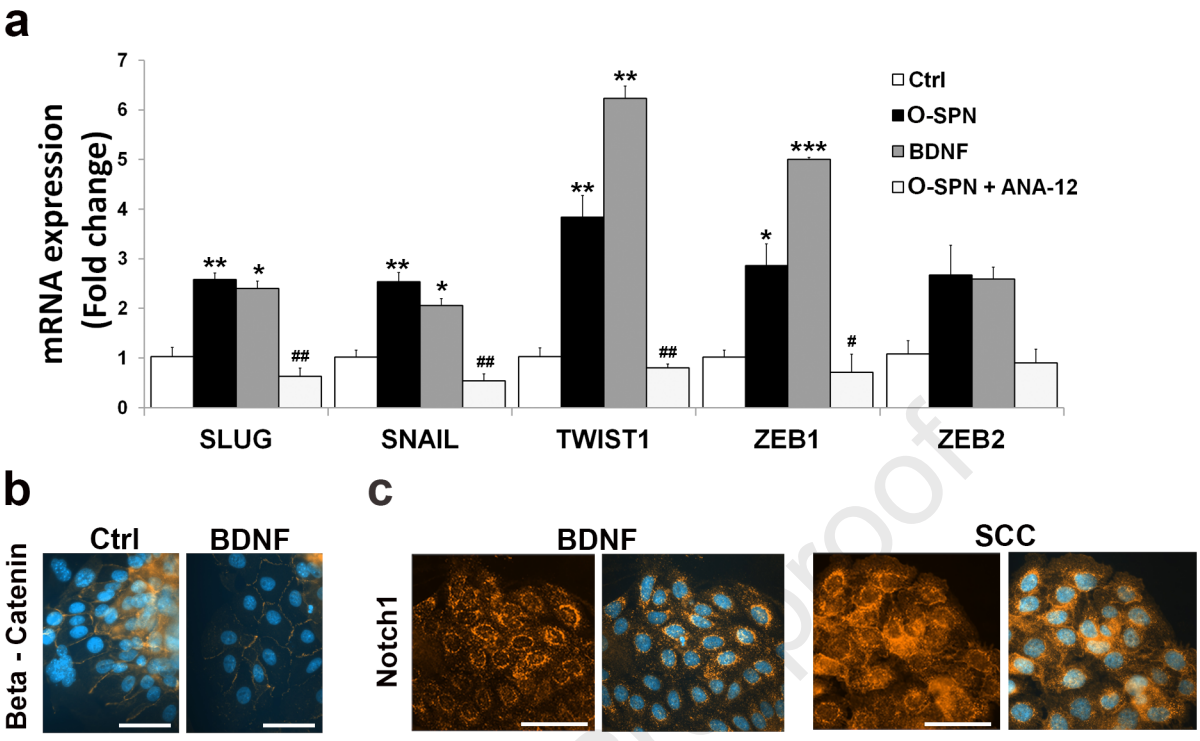

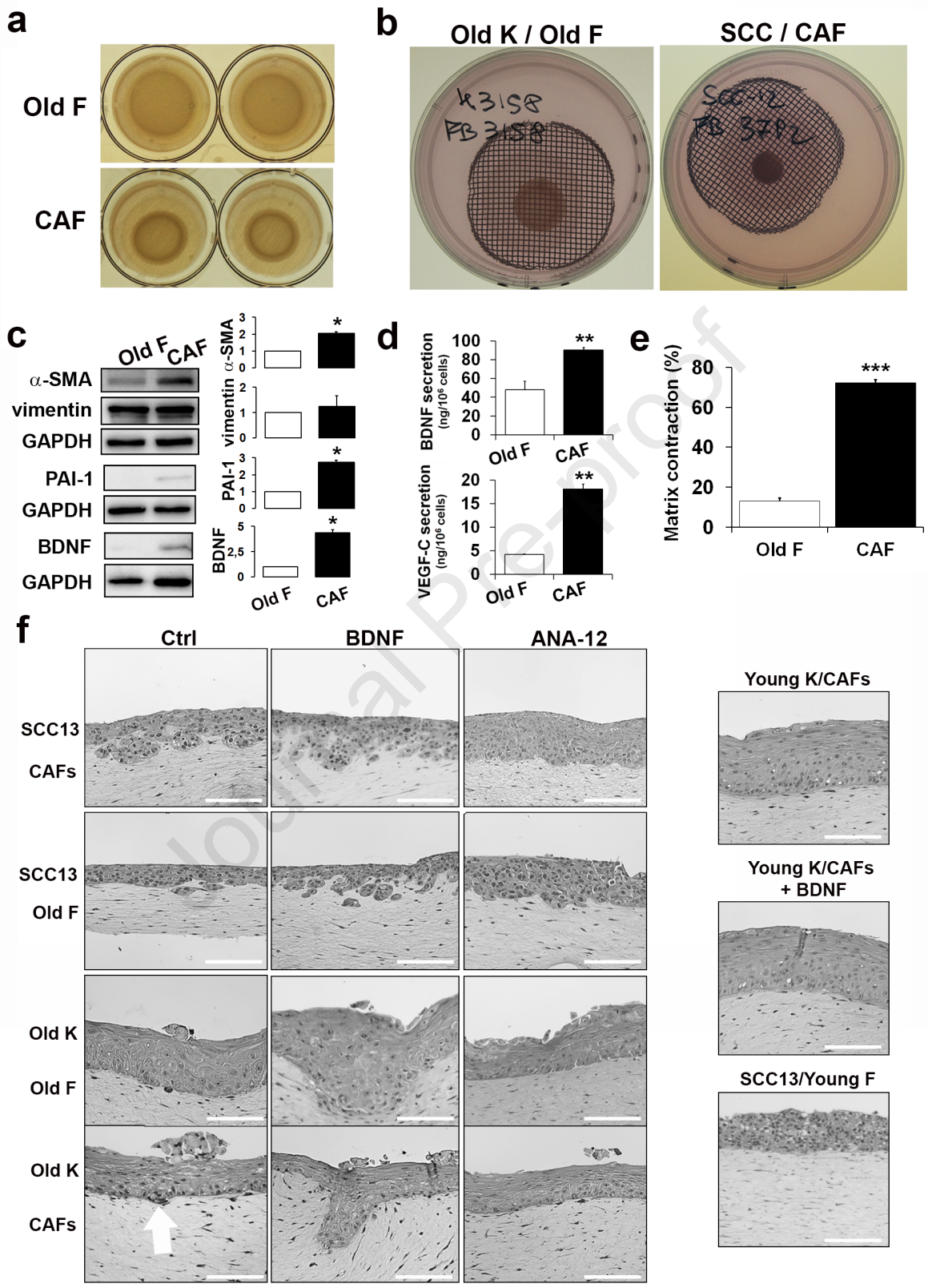

SUPPLEMENTARY MATERIALS AND METHODS

Cell culture, colony forming efficiency and population doublings

Human keratinocytes and fibroblasts were obtained from skin biopsies of three healthy young (< 10 years) and three old (>70 years) donors and cultivated on a feeder-layer of lethally irradiated 3T3-J2 cells (Rheinwald and Green 1975; Panacchia et al. 2010). Procedures were performed in accordance with the ethical standards of the Committee on Human Experimentation of IDI-IRCCS. The study was conducted according to the principles of the Declaration of Helsinki.

3T3-J2 cells (a gift from prof. Howard Green, Boston, MA), primary human keratinocytes and fibroblasts were grown as described previously (Panacchia et al. 2010). Human CAF isolated from patients with cutaneous SCC were grown in DMEM supplemented with 10% FCS. SCC13 and 15 cells (a gift from James Rheinwald, Boston, MA) were grown as described previously (Rheinwald and Beckett 1981)

Colony Forming Efficiency (CFE) assay was performed as previously described (Maurelli et al. 2006). Keratinocyte and fibroblast cultures were serially cultured. Number of cell doublings were calculated according to the formula x = 3,322 log N / N0 (N = total number of cells obtained at each step; N0 = total number of plated cells x CFE).

For further experiments, cells have been used at 2nd culture passage. Specifically, primary keratinocytes from young and old donors have been used 12.01±1.47 and 12.79±1.30, respectively. Primary fibroblasts from young and old donors have been used at 6.15±0.33 and 5.46±0.19, respectively.

Culture treatments

SPNs were obtained from primary fibroblasts at 70% of confluence cultured in DMEM, glutamine 2% for 72h. SPN was collected, clarified by centrifugation and stored at -80°C for further analyses. Human recombinant BDNF and monoclonal anti-human BDNF (Sigma-Aldrich) and TrkB inhibitor ANA-12 (Cayman Chemical) were used at the final concentration of 50ng/ml, 1µg/ml and 50µM, respectively. Recombinant Human NT-3 and NT-4 were from Peprotech.

Keratinocyte were seeded onto feeder-layer, cultured for 48h in complete medium (DMEM, Ham's F12, 10% fetal bovine serum, 50 IU-50 µg/ml penicillin-streptomycin, 4 mM glutamine, 5 µg/ml insulin, 0.18 mM adenine, 0.4 µg/ml hydrocortisone, 0.1 nM cholera toxin, 2 nM tri-iodothyronine). Cultures were treated for 7 days with medium replacement every two days. Culture treatments were performed in basal medium (keratinocyte complete medium depleted of fetal calf serum, cholera toxin, and containing 10 ng/ml insulin)(Di Marco et al., 1993), which

correspond to control (Ctrl) treatment, or 1/4 v/v basal medium (4x) supplemented with 3/4 v/v of SPN, BDNF, SPN+ANA-12 or SPN+anti-BDNF specific antibody. Although keratinocyte growth was slow down in basal medium compare to complete medium, cells are able to differentiate, stratify and form regular colonies. Subconfluent cultures were used for CFE, immunoblot or RTqPCR analysis.

Keratinocytes were seeded on round coverslips onto feeder-layer, cultured for 48h in complete medium and then treated. For proliferation assay, EdU was incubated for 24h and then cells were fixed. For immunofluorescence, cells were fixed 24h following treatments.

Fibroblast secretome analysis

Collected fibroblast SPNs were submitted to three biotin-label-based antibody arrays for profiling of protein secretion (RayBio C-Series Human Cytokine Antibody Array C6, C7, and MMP, RayBiothec, Norcross, GA). Protein levels were evaluated by densitometric analysis by a GS-710 scanner and Quantity One software (Bio-Rad). Data analysis was performed as described previously (Huang et al. 2010).

BDNF and VEGF-C levels were measured by Total BDNF and VEGF-C Quantikine ELISA Kit, respectively (R&D Systems Europe, Ltd).

Quantitative RT-PCR

RNA was extracted from cells by TRIzol (Invitrogen). Total RNA was reverse transcribed by an oligo(dT) primer (Invitrogen). mRNA levels were analyzed by a QuantiTect SYBR Green-PCR kit (QIAGEN) by an ABI PRISM 7000 (Applied Biosystems). mRNA levels were normalized by GUSB gene as housekeeping gene. Primers are shown in Table S1.

To analyze selected genes related to cellular senescence and cancer stem cell, total RNA was reverse transcribed by the reverse transcriptase kit RT^2 First Stand Kit (Qiagen) and multiple qRT-PCR were performed by RT^2 Profiler PCR Array (Qiagen).

Relative quantities of mRNA expression levels were calculated according to $2^{-\Delta Ct}$ method (for receptor expression) (Scardocci et al. 2006) or $2^{-\Delta\Delta Ct}$ method.

Proliferation assay

The proliferation assay was performed by the Click-iT® EdU Alexa Fluor® 488 Imaging Kit (Thermo Fisher). Treated cultures were incubated with EdU for 24 hours and nuclei were counterstained with Hoechst. All nuclei of 10 random fields (around 5000 nuclei)/treatment were counted and proliferating cell percentage was calculated as EdU-positive / Hoechst stained nuclei.

SA-beta-galactosidase assay was performed by staining kit (Thermo Fisher).

Tyrosine-phosphorylation of human TrkB assay

Tyrosine-phosphorylation of human TrkB was measured in cell lysates using DuoSet® IC ELISA kit (R&D Systems Europe, Ltd). Keratinocyte cultures were treated with BDNF for 15' and lysated following manufacturer instructions.

Immunofluorescence

Cells were fixed in 4% paraformaldehyde and immunofluorescence was performed as previously described (Maurelli et al. 2016). Antibodies are shown in Table S2. Nuclei were stained with DAPI. The quantification of protein expression/cell was evaluated in 10 colonies/treatment. Images were captured with the ApoTome System connected with Zeiss Axiovert200 inverted microscope. Image analysis was performed with ZEN softwares (Zeiss).

Immunoblot analysis

Subconfluent keratinocytes were extracted as previously described (Maurelli et al. 2016) and equal amounts of samples were electrophoresed on 7.5–12.5% SDS-polyacrylamide gels. Immunoblotting was performed as described previously (Maurelli et al. 2016). Antibodies are shown in Table S2. Protein levels were evaluated by densitometric analysis by a GS-710 scanner and QuantityOne software (Bio-Rad) and then normalized to GAPDH protein levels.

Soft agar assay

Single cells were mixed thoroughly in 0.3%-agar-containing complete medium (Agar Noble (BD Biosciences) dissolved in keratinocyte growth medium) and seeded in 10 cm-diameter plates over a 0.5% agar layer. After 21 days, colonies were counted for each plate. Each soft agar assay was performed in triplicate.

Keratinocyte migration assay

Migration was evaluated by OrisTM Cell Migration Kit (Platypus Technologies). Cells were seeded at high density ($5x10^4$/well) into 96-well plates containing silicon stoppers that restrict cells into an outer annular region and serum-starved over-night. The day after, stoppers were removed and cells were treated. Each well was photographed by EnSight Multimode Plate Reader at different time. Cell-free area was measured by ImageJ software. The percentage of gap closure was calculated as [1- (cell-free area T/cell-free area T0)*100]

Organotypic invasion assays

For 3D organotypic culture generation, 5×10^5 fibroblasts or CAF were embedded in 1-ml matrix gel. After 1h at 37 °C, gels were overlaid with 5×10^5 SCC13 cells or primary keratinocytes. 3D models were lifted at the cell-air interface 24 h later, treated for 5 days and then fixed. Quantification of the Invasion Index (I.I) was assessed measuring specific area of paraffin-embedded sections of 3D models stained with H&E by ImageJ software. I.I was calculated as 1 – (non-invading area/total area) (Albrengues et al. 2015).

Matrix contraction assay

Collagen lattices with embedded fibroblast or CAF were made as above described. Surface area of gel was measured at T0 and after 72h. Gel area was measured by ImageJ software. The gel contraction was expressed as percentage of the initial non-contracted area following the formula: [1- (A2/A1)*100], where A1 is the initial gel area and A2 the area after 72h.

Statistical analysis

Data were expressed as mean±standard deviation (s.d). Statistical analysis was performed by the Student's t-test. Differences were considered statistically significant at $P < 0.05$.